Journal of Soils and Sediments (2024) 24:1103–1123
https://doi.org/10.1007/s11368-023-03701-w

SOILS, SEC 2 • GLOBAL CHANGE, ENVIRONMENTAL RISK ASSESSMENT, SUSTAINABLE LAND USE • RESEARCH ARTICLE

Influence of biochar on the soil-water retention behavior of compacted loess in man-made earth structures in loess regions

Liang Sun[1] · Ping Li[1,2] · Wenbin Fei[3] · Jiading Wang[1]

Received: 16 August 2023 / Accepted: 3 December 2023 / Published online: 4 January 2024

Abstract

Purpose The objective of this study was to investigate the influence of apple tree biochar on the soil water retention curve (SWRC) of compacted loess, which is increasingly used in man-made earth structures in loess regions. Additionally, we aimed to elucidate the underlying mechanisms from both physicochemical and microstructural perspectives and propose potential directions for future research.

Materials and method Compacted biochar-amended loess (BAL) specimens with different biochar contents, dry densities or molding water contents were prepared, and their SWRCs were determined. Besides, the hydrophilicity, minerals, functional groups, structure and pore-size distribution (PSD) of loess, biochar and BALs were characterized for exploring the mechanisms by which biochar modifies the SWRC of loess.

Results and discussion The addition of biochar significantly improves the water retention capacity of compacted loess. With the increase of biochar content, both the saturated water content and air-entry value (AEV) increase, and the desaturation rate slightly increases. The influence of molding water content and dry density on the SWRC of BAL is similar to that on the SWRC of compacted loess.

Conclusions On the one hand, the apple tree biochar studied is highly hydrophilic due to the presence of abundant oxygen-containing functional groups and negative charges on its surfaces, thus significantly enhancing the soil wettability. On the other hand, the biochar addition increases the volume of inter-aggregate pores and changes the type and size of aggregates, aggregates with a wide range of sizes are arranged more closely in BAL. Therefore, the soil water retention capacity and drainage capacity are improved. This study provides a theoretical basis for the applications of biochar in geotechnical or geo-environmental engineering in loess regions, however, further investigations are imperative.

Keywords Biochar-amended loess · Compacted loess · Soil-water retention curve · Pore structure · Hydrophilicity · Functional groups

1 Introduction

Global carbon emissions from energy combustion and industrial processes have increased by 50% from 1990 to 2022, reaching nearly 321 million tons annually, as reported by the International Energy Agency in 2023 (IEA 2023). This could exacerbate the global climate change and increase the frequency and severity of extreme natural disasters, such as typhoons, extreme droughts, torrential rains, mudslides and landslides. These events have a detrimental impact on both the Earth's ecosystem and people's lives (Park and

Responsible editor: Mohammad Valipour

✉ Ping Li
liping_dzxx@nwu.edu.cn

Liang Sun
202121960@stumail.nwu.edu.cn

Wenbin Fei
wenbin.fei@unimelb.edu.au

Jiading Wang
wangjd@nwu.edu.cn

[1] State Key Laboratory of Continental Dynamics, Department of Geology, Northwest University, Xi'an, China 710069

[2] Water Cycle and Geological Environment Observation and Research Station for the Chinese Loess Plateau, Ministry of Education, Zhengning, Gansu, China 745399

[3] Department of Infrastructure Engineering, The University of Melbourne, Parkville, Australia

Kug 2022). In recent years, many countries and organizations have taken concrete actions to be carbon neutral for climate change mitigation and sustainable development (e.g., Mallapaty 2020; Williams et al. 2021; Huovila et al. 2022). Biochar is a carbon-rich solid material obtained by pyrolyzing (or gasifying, torrefying, carbonizing) biomass (such as woodchips, crop residues, animal manures and sewage sludges) at a high temperature (300 – 1000 ℃) under low or anoxic conditions (Lehmann and Joseph 2015) (Fig. 1). Because of its biomass feedstock, biochar has a high carbon content of up to 60% (Lehmann and Joseph 2015). It was also reported that biochar exhibits greater persistence than its feedstock due to the specific molecular configuration (strongly bonded carbon atoms) (Edeh et al. 2020) and thus has a longer half-life (over 100 years). Therefore, biochar has been used as a sustainable soil amendment to increase the organic carbon, organic matter or humus content of soil, helping achieve carbon sequestration, enhance soil nutrients and increase crop yields (Chen et al. 2019) (Fig. 1). In addition, the light weight and porous structure of biochar resulting from its unique processing technology enable it to be used for mitigating environmental risks such as municipal wastewater treatment and improving soil properties in man-made earth structures. As this lightweight, granular and porous solid material is gradually introduced into soil, increasing attention has been paid to the soils amended with biochar. The physicochemical properties such as specific gravity and pH (e.g., Abel et al. 2013; Gul et al. 2015; Garg et al. 2021), hydraulic properties such as water retention capacity and permeability (e.g., Jeffery et al. 2015; Wong et al. 2018; Liu et al. 2022), mechanical properties such as shear strength and compressibility (e.g., Reddy et al. 2015; Zong et al. 2016; Hussain and Ravi 2022) of various biochar-amended soils were examined by scholars from different fields (Fig. 1).

Biochar is generally considered to have a porous structure, low specific gravity, large specific surface area (SSA), high cation exchange capacity (CEC), and abundant surface functional groups (Wang and Wang 2019; Chen et al. 2019). In fact, the physicochemical properties of biochar are influenced by its feedstock (e.g., type, structure, and contents of hemicellulose, cellulose, and lignin in biomass) and pyrolysis condition (e.g., pyrolysis temperature, heating rate and heating time) (Lehmann 2007; Hussain et al. 2020a; Anand et al. 2022). For example, wood-based biochar has a more porous structure, lower specific gravity, and higher SSA compared to manure/biosolid-based biochar (Tomczyk et al. 2020); while manure/biosolid-based biochar generally has a higher ash content, pH, and CEC compared to crop waste- and wood-based biochar (Yuan et al. 2011). The pyrolysis temperature can have a significant influence on the structure and wettability (hydrophilicity or hydrophobicity) of

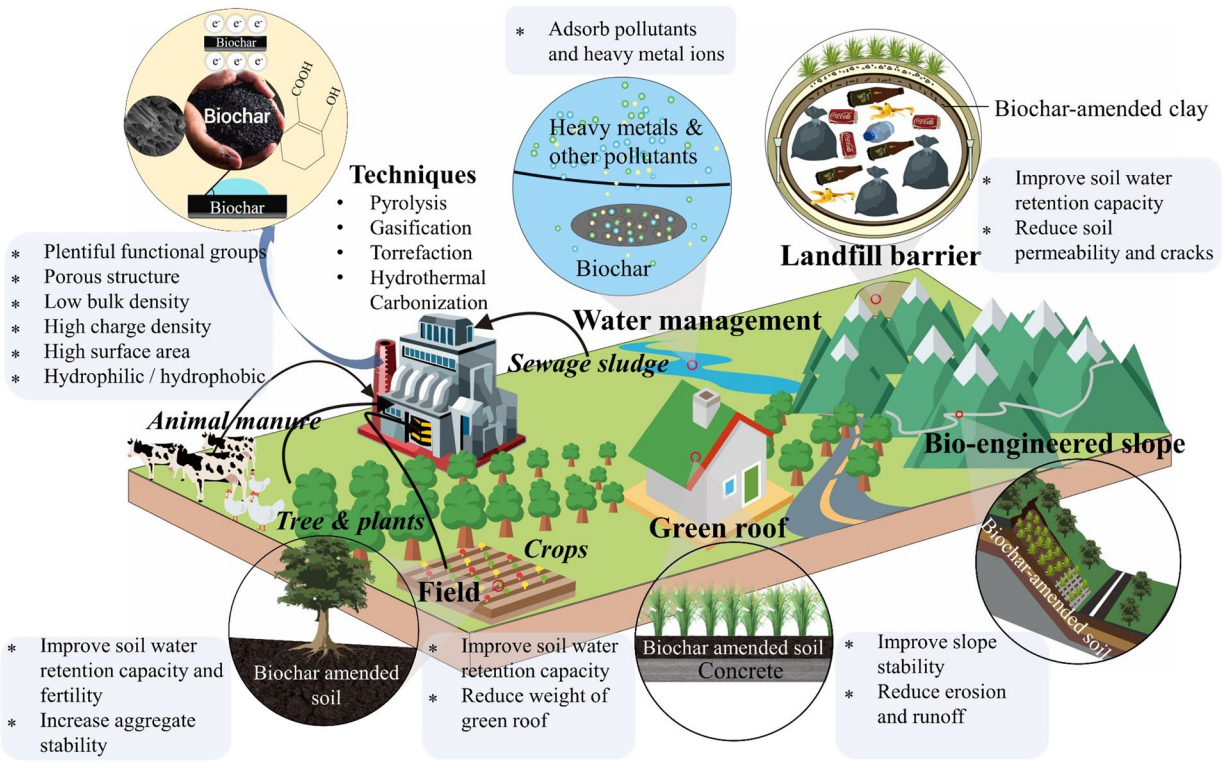

Fig. 1 Production, properties, and applications of biochar

biochar. As the pyrolysis temperature increases, aliphatic functional groups are volatilized and lost (Novak et al. 2009; Yuan et al. 2011; Chintala et al. 2014; Gul et al. 2015), resulting in a more porous structure and increased hydrophilicity (Bansal et al. 1988; Al-wabel et al. 2013); concurrently, the aromaticity of biochar is also increased, which increases the hydrophobicity of biochar. The wettability of biochar depends on the relative changes in functional groups and aromaticity (Lian et al. 2011; Lu et al. 2023). In summary, the properties of biochar pyrolyzed from diverse feedstocks or at diverse temperatures can vary dramatically; these properties, including the SSA, ionic and mineral composition, specific gravity, pH, CEC, and surface functional groups, affect the interaction between biochar and soil. As a result, the engineering properties of biochar-amended soil are influenced (Uzoma et al. 2011; Igalavithana et al. 2017; Tomczyk et al. 2020; Zhang et al. 2021).

Reaching a consensus on the influence of biochar on the water retention capacity of soil is probably impossible, mainly owing to the diverse nature of biochar and soil (Lu et al. 2023). It can be summarized into two groups (biochar- and soil-related) and most factors within each group are interdependent (e.g., Ippolito et al. 2020; Zhang et al. 2021; Alghamdi et al. 2020; Gluba et al. 2021). Thus, four factors can mainly be dependent on, namely, 1) soil type, particle size or density, which indicates the composition and structure of soil, 2) specific gravity or SSA of biochar, which indicates the porosity, structure and ash content of biochar, 3) wettability of soil and biochar, the former one varies with soil type and properties (e.g., the water, clay and organic matter content, pH, the presence of fungal mycelium and others), the latter one depends on the relative quantity of hydrophobic and hydrophilic functional groups and aromaticity, 4) suction level. A summary of recent studies on the soil-water retention curve (SWRC) of biochar-amended soil is presented in Table S1 in the supplement. It shows that biochar generally improves the water retention capacity and increases the saturated water content of sandy soil (which has been extensively studied, e.g., Abel et al. 2013; Sun and Lu 2014; Jeffery et al. 2015; Suliman et al. 2017; Hussain et al. 2020b; Chen et al. 2022a), while has little effect on the water retention capacity of silty soil (Ouyang et al. 2013; Mao et al. 2019), and even reduces the water retention capacity of clayey soil (Sun and Lu 2014; Kameyama et al. 2016). The water retention capacity of sandy soil was also reported to be reduced by biochar. For instance, Suliman et al. (2017) found that pine wood biochar improved the water retention capacity of a sandy soil, whereas pine bark biochar decreased its water retention capacity. The influences are opposite because pine wood biochar is hydrophilic, whereas pine bark biochar is hydrophobic. This indicates that although wood-based biochar provides additional spaces for retaining water and reduces the average pore size, the wettability of biochar plays a crucial role in influencing the SWRC. Another example is peanut shell biochar, which has been reported to enhance the water retention capacity of both silty sand (Ni et al. 2018; Chen et al. 2022b) and kaolin (Wong et al. 2017, 2022). In addition, the influence of biochar on the SWRC may vary with the suction level. To be specific, the soil water retention capacity could be improved in the high suction range when micropores are increased due to biochar application, while the improvement could be observed in the low suction range when macropores are increased. However, peanut shell biochar was observed to increase the water retention capacity of kaolin in both the low suction range (< 1000 kPa) and high suction range (48.49 – 124.56 MPa) (Wong et al. 2017, 2022). Similar results were obtained for water hyacinth biochar, which was reported to increase the water retention capacity of silty sand in both the low suction range (< 3000 kPa) (Hussain et al. 2020b) and high suction range (10 – 100 MPa) (Huang et al. 2021). Therefore, we consider the wettability of biochar, as well as the difference in the particle or pore size between biochar and soil to be responsible; and the difference in wettability or hydrophilicity between soil and biochar largely determines the biochar-induced modifications of the SWRC.

Research on the hydraulic properties of biochar-amended soil is still in its early stages, especially for loess soils. Firstly, most related studies aimed at the soil tillability and plant growth, with particular attention given to determining the soil moisture at low suctions, such as the field capacity and wilting point since the amount of water available for plants is concerned (e.g., Ouyang et al. 2013; Sun and Lu 2014; Castellini et al. 2015; Kameyama et al. 2016; Rasa et al. 2018). However, soils may experience extreme droughts and produce high suctions in practice, especially in geotechnical or geo-environmental engineering (such as landfill covers, engineered slopes and embankments), the water retention and associated mechanical behavior (e.g., desiccation cracking) are therefore of great significance (e.g., Bordoloi et al. 2018; Lu et al. 2021). Besides, the SWRC used for modeling the seepage is always obtained by fitting many measured data points with a known mathematical equation, the number of data points and measurement range of suction undoubtedly influence the accuracy of SWRC in numerical calculation (Zapata et al. 2000; Li et al. 2018). Secondly, biochar has already been used in geotechnical or geo-environmental engineering, such as landfill covers and man-made filled slopes, because it can enhance plant growth and alleviate cracking (Chen et al. 2016, 2018; Ng et al. 2022). Whereas, there is a lack of studies focusing on biochar-amended loess (BAL) under high compaction conditions, despite the fact that engineered slopes and other man-made earth structures often require such conditions. This limits the potential applications of biochar in geotechnical or geo-environmental engineering in loess regions.

Therefore, a comprehensive understanding of the SWRC of densely compacted BAL is urgently needed, which will serve as a theoretical basis for the applications of biochar in geotechnical or geo-environmental engineering in loess regions.

In this study, the SWRC of compacted BAL was investigated. Besides, the hydrophilicity, minerals, functional groups, structure and pore-size distribution (PSD) of loess, biochar and BALs were characterized to gain a deep and comprehensive insight into the mechanisms by which biochar modifies the SWRC of loess. Our hypothesis is that biochar can increase the water retention capacity of compacted loess since its porous structure provides additional spaces for water retention.

2 Materials and methods

2.1 Materials

The loess tested was collected from Binzhou, Shaanxi, China at a depth of 4–6 m below the ground, and its physical properties measured using intact block samples following relevant ASTM standards are summarized in Table 1. The liquid limit and plasticity index are 27.81% and 11.55, it can be classified as a low plastic clay (CL) according to the Unified Soil Classification System (ASTM 2013). The biochar used was purchased from Shaanxi Yixing Technology Co., Ltd. and it was produced by pyrolyzing apple trees and branches at a temperature of about 550 °C. This biochar was selected because the apple tree planting area in the Loess Plateau, which has been maintained at about 20,000 hectares in the past 10 years, accounts for 55.2% of the total apple tree planting area in China (China Statistical Yearbook 2020). Increasing planting area, pruning and other agricultural activities generate a large amount of waste (i.e., apple trees and branches) that can provide abundant raw materials for the production of biochar. Undoubtedly, converting these agricultural wastes into biochar and returning them to loess soils for both agricultural and geo-environmental purposes is an effective approach to sustainable development. Basic physicochemical properties of the biochar derived from apple trees are listed in Table 2.

Table 1 Physical properties of the loess studied

Physical property	Value
In-situ density (g/cm^3)	1.37
Specific gravity, G_s	2.68
Plastic limit, w_p (%)	16.26
Liquid limit, w_L (%)	27.81
Plasticity index, PI	11.55
Optimum water content (%)	18.00
Maximum dry density (g/cm^3)	1.63

The air-dried loess was screened with a 2 mm sieve and the biochar was screened with a 0.5 mm sieve, and then both were dried at 105 ℃ for 24 h. After both materials were cooled to the room temperature, the biochar and loess were removed from the oven and mixed with different mass ratios of biochar to loess (i.e., biochar content, 0%, 5%, 10%, 20%). These contents were chosen because the biochar content was less than 20% in almost all of the studies related to biochar-amended soils (e.g., Wong et al. 2017, 2022; Zhang et al. 2020; Hewage et al. 2023). The Atterberg limits of biochar-loess mixtures were measured, as summarized in Table 3 (where, BAL is short for biochar-amended loess; C denotes the biochar content, i.e., mass ratio of biochar to loess). It can be seen that with the increase of biochar content, both the plastic limit and liquid limit of biochar-loess mixture are increased, and the plasticity index exhibits an increase upon the addition of biochar, while showing little variation as the biochar content is further increased. In addition, the compaction curves of loess and biochar-loess mixtures were determined by conducting Standard Proctor Compaction tests (ASTM D698-12 2012), as shown in Fig. 2a. The optimum water content is increased while the maximum dry density is decreased in response to the addition of biochar, as summarized in Table 3.

2.2 Specimen preparation

Compacted specimens were used for the SWRC characterization, the graphical depiction of the step-by-step procedure for specimen preparation can be found in Fig. 3. Firstly, the soil blocks extracted in the field were crushed, ground, air-dried and screened with a 2 mm sieve; and the purchased biochar was screened with a 0.5 mm sieve. Both materials (loess and biochar) were oven-dried. Then, the soils were divided into parts and each part was mixed with a certain amount of biochar to achieve a predetermined mass ratio of biochar to loess (i.e., 0%, 5%, 10%, or 20%); the mixture was fully stirred until the color became uniform (the loess is buff-colored and the biochar is dark). After that, a certain amount of distilled water was sprayed onto the mixture to reach the desired molding water content (i.e., mass ratio of water to solid particles, 14%, 18%, or 22%). The wet mixtures were sealed in plastic bags and stored in humid

Table 2 Physicochemical properties of the purchased biochar

Property	Value	Source
pH	9.52	Li et al. (2020a)
Ash content (%)	13.16	Li et al. (2020a)
Organic C(g/kg)	467.47	Li et al. (2020a)
C/N	82.30	Han et al. (2022)
SSA(m^2/kg)	1.05	Li et al. (2020a)

Table 3 Physical properties of BALs

Specimen	Specific gravity G_s	Plastic limit w_p (%)	Liquid limit w_L (%)	Plasticity index PI	Optimum water content (%)	Maximum dry density (g/cm^3)
Loess	2.68	16.26	27.81	11.55	18.00	1.67
BAL-C5	2.58	18.30	33.54	15.24	20.00	1.61
BAL-C10	2.57	19.19	34.34	15.15	21.64	1.53
BAL-C20	2.55	22.11	37.86	15.75	28.00	1.36

chambers for at least 72 h for water equalization. Finally, each mixture was compacted statically using a self-designed specimen preparation equipment to reach the dry density of 1.4 g/cm^3, 1.5 g/cm^3, or 1.6 g/cm^3. A total of 72 BAL specimens were prepared for the SWRC measurement using the axis translation technique, they had different biochar contents (BCs) or molding water contents (MWCs) or dry densities (DDs), and were 1 cm in height and 4 cm in diameter, as shown in Fig. 3. Each specimen has its duplicates.

2.3 SWRC measurement

A 15-bar pressure plate extractor was used for the measurement of SWRC, as shown in Fig. 3. Once the BAL specimens were prepared, they were saturated, weighed, and placed onto the pre-saturated ceramic disk in the pressure chamber with a wet filter paper beneath each specimen. Then, an air pressure regulated by the pressure control system was applied to the chamber to achieve a predetermined

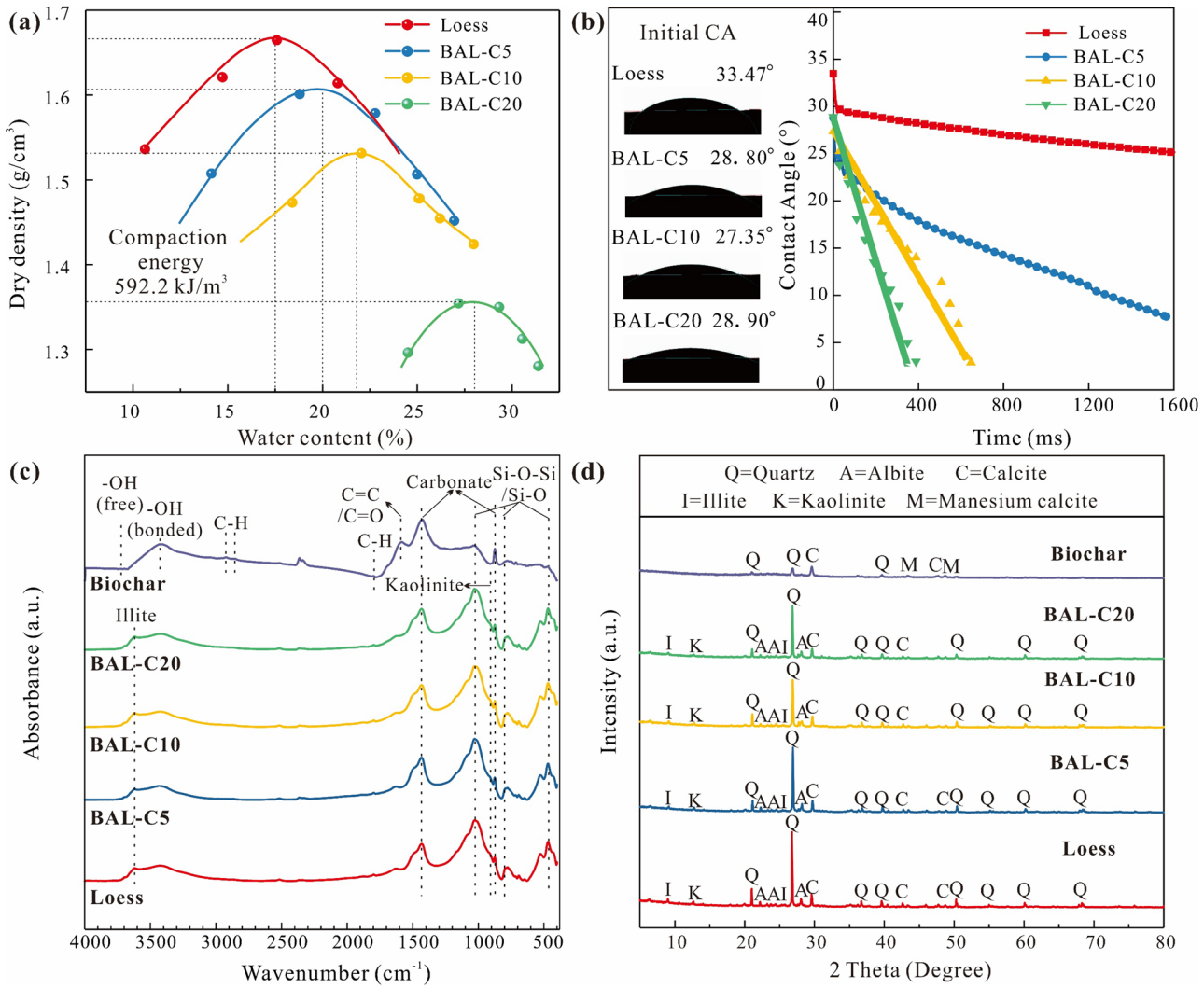

Fig. 2 Physicochemical properties of biochar, loess and BALs: **a** compaction curves, **b** variation of contact angle, **c** FTIR spectra and **d** XRD spectra

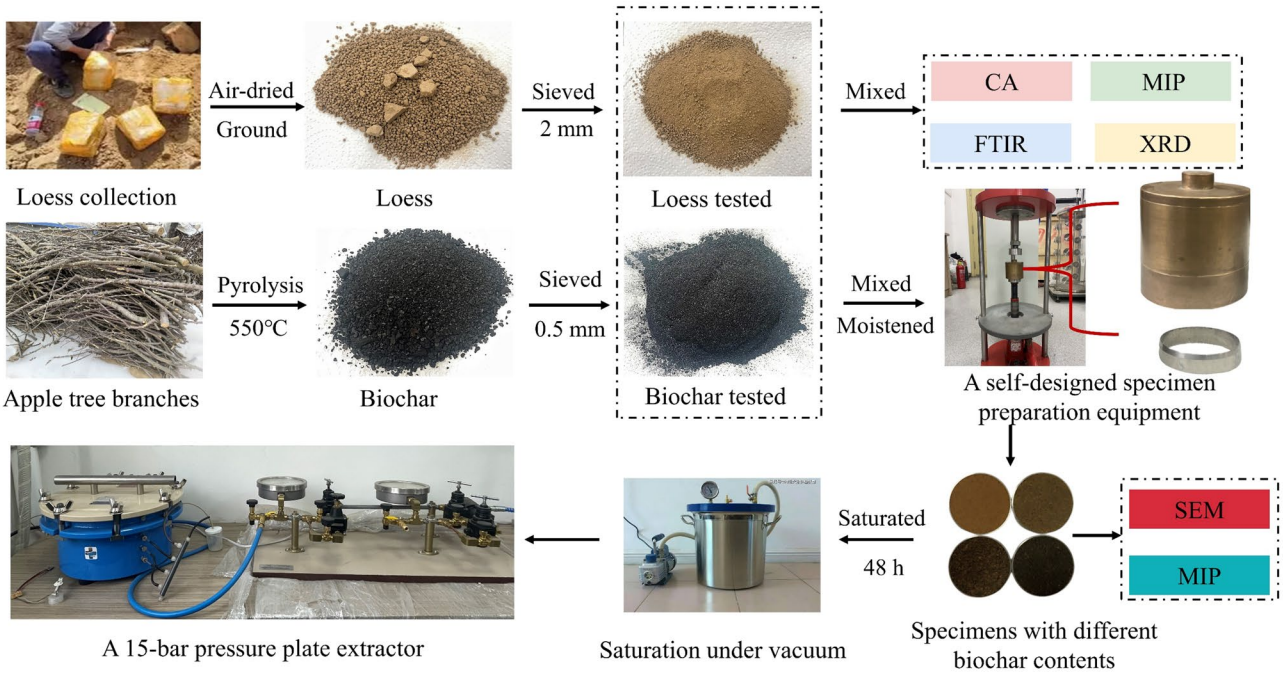

Fig. 3 Specimen preparation for various tests

matric suction (thereafter referred to as suction, equal to the air pressure applied to the specimens since the water phase is connected to the atmosphere, i.e., axis translation technique), in order to desaturate the BAL specimens gradually. The air pressures applied to the chamber or specimens were successively 1, 3, 6, 10, 25, 50, 75, 100, 150, 200, 300, 400, 500, 700, 900 and 1100 kPa (Xiao et al. 2022). As the air pressure or suction in the chamber increased, water drained from the BAL specimens until reaching the equilibrium. Under different suction values, the time required for the equilibrium varied, usually between 4 and 14 days. The higher the suction was, the longer the time was required. Once the equilibrium was achieved under each suction (no water outflowing from the chamber or specimens), the BALs were removed from the chamber and weighed on a balance with the accuracy of 0.0001 g, to determine their gravimetric water contents (hereafter referred to as water contents).

During the test, since specimen was removed from the pressure plate extractor and weighed on a balance once the soil moisture reached the equilibrium, the solid mass of the specimen would change if the specimen was taken to the balance and then put back to the extractor a dozen times. For example, a very small amount of soil particles would remain on the filter paper which was placed beneath the specimen, especially at high degrees of saturation, or on the tray of balance during weighing. Moreover, saturating specimen under the vacuum condition before the SWRC measurement would result in a loss of solid mass, especially at high biochar contents. In the test, the specimen was weighed under each suction to compute the mass of water discharged by the specimen. After the test, the specimen was oven-dried to determine the mass of solid particles and water content of the specimen under final suction. We compared the solid mass after the test with that of the as-compacted specimen and found the difference was less than 1.0 g. So, the average of two values was regarded as the mass of solid particles, and water content of the specimen under each suction was obtained by dividing the corresponding amount of water discharged from the specimen by the mass of solid particles. In a word, it was more convenient to express the SWRCs in terms of gravimetric water content, and the measured gravimetric water content can be converted into volumetric water content without considering any change in soil volume.

2.4 Microstructural characterization

The prepared BAL specimens were freeze-dried prior to the microstructural characterization using either MIP or SEM, to minimize the structural disturbance during the drying process (Romero et al. 1999). After that, the freeze-dried BAL specimens were cut into cubes with an appropriate size, $1 \times 1 \times 2$ cm^3. An AutoPore IV 9500 porosimeter was used to characterize the pore-size distribution (PSD) of BAL. The porosimeter is capable of exerting a pressure ranging between 0.5 and 60,000 psi on mercury, causing it to intrude into

the pores progressively, from the larger to the smaller, as the pressure increases progressively. According to the law of capillarity, the pores with an entrance diameter between 3 nm and 360 µm were detectable (Washburn 1921). Besides, the BAL specimens were directly observed using a Quanta 450 scanning electron microscope to analyze their structural characteristics, including the size of particles or aggregates, contact between particles or aggregates, size and morphology of pores, and so on. A freeze-dried $1 \times 1 \times 2$ cm^3 specimen was fractured at mid-height, and a fresh section was sputter-coated with platinum (i.e., Pt) before being observed using the microscope. Various magnifications and representative views were selected for shooting. Figure 4 displays the biochar particles in BAL, which have a vascular bundle structure (Tan et al. 2015).

2.5 Measurement of surface properties

The hydrophilicity of loess, biochar and BALs were assessed by measuring their contact angles, while the functional groups of biochar, BALs and loess were identified using the Fourier Transform Infrared Spectrometry (FTIR) technique. Additionally, their mineral compositions were investigated using the X-ray Diffraction (XRD) technique. The results of loess, biochar and BALs were used for comparative analysis to examine the potential modifications of surface properties of loess induced by biochar application, to disclose the mechanisms by which biochar influences the SWRC of compacted loess.

The contact angle measurements were conducted to characterize the hydrophilicity of loess, biochar and BALs. A Dataphysics-OCA20 Optical Contact Angle Meter which includes an optical system, a video system and various analytical software was used. In the test, the process as a 3-µL water droplet was dropped onto the sample until it infiltrated the sample was recorded, and the contact angle was determined by the analytical software. Figure 2b illustrates the variation of contact angles of loess and BALs with time. The material is considered hydrophilic when the initial contact angle is less than 90°, otherwise the material is hydrophobic (Liu et al. 2022). From Fig. 2b, it can be observed that loess, biochar and BALs are hydrophilic since their initial

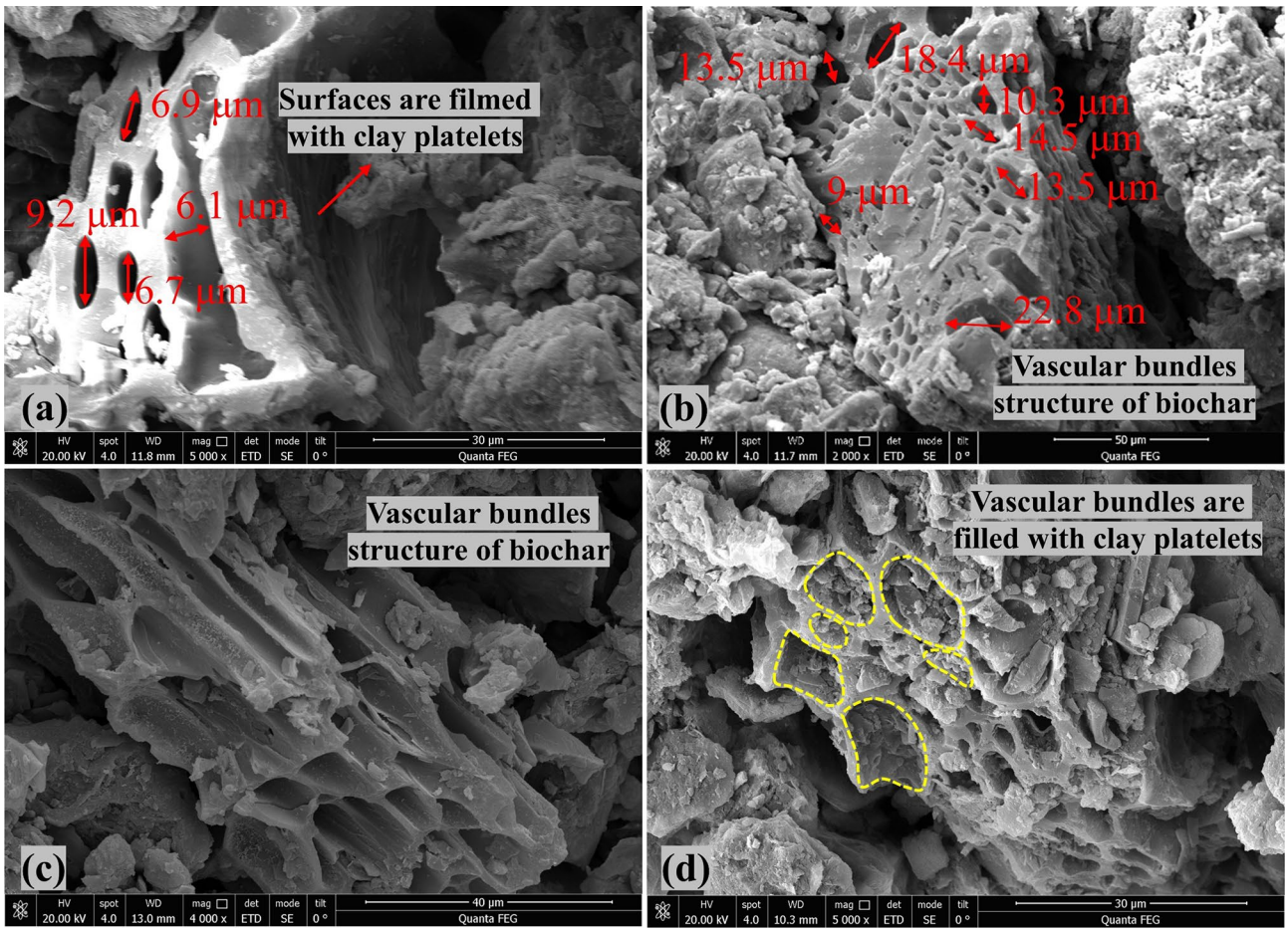

Fig. 4 Micrographs of biochar

contact angles are all less than 90°. The higher the biochar content, the smaller the contact angle of BAL. It suggests that the addition of biochar enhances the soil hydrophilicity and this effect is positively correlated with the amount of biochar added. The contact angle of biochar was measured and considered to be zero, since when a 3-μL water droplet was dropped onto the sample it infiltrated too quickly to be captured and quantified by the digital camera of the contact angle meter.

The functional groups and minerals on the surfaces of solid particles were characterized using the FTIR technique (Igalavithana et al. 2017). This technique uses infrared light with varying frequencies to illuminate compounds, inducing molecular transitions between vibrational energy levels and generating infrared absorption spectra, thereby facilitating the identification of functional groups in compounds according to the enhancement or attenuation of infrared light. The infrared spectra of biochar, BALs and loess at the intermediate and far infrared region (4000 – 650 cm^{-1} and 650–450 cm^{-1}) are presented in Fig. 2c. For the biochar derived from apple trees and branches, the peaks (indicating high absorbance) at the wavenumber of 3500 – 4000 cm^{-1}, 2882 – 2972 cm^{-1}, 1590 – 1610 cm^{-1} are attributed to -OH, C-H and C=C/C=O functional groups, respectively (Han et al. 2022). In addition, the peaks at 1445 and 877 cm^{-1} are due to the presence of carbonates (Wang et al. 2020; Han et al. 2022), and the peaks at 470, 800, and 1031 cm^{-1} represent Si-O/Si-O-Si bonds in quartz (Wang et al. 2020; Han et al. 2022). Similar results were obtained for loess and BALs, which could be attributed to the wrapping of biochar with clay partciles in BAL (this will be further discussed later). Their spectrums appear to peak at 912 and 3622 cm^{-1}, indicating the presence of kaolinite and illite, respectively (Wang et al. 2020; Liu et al. 2022).

The XRD technique was utilized to determine the minerals in biochar, loess and BALs (Igalavithana et al. 2017). This technique enables the identification of multiple crystals in materials based on their unique diffraction patterns, as each crystal has its unique structure, resulting in a distinctive diffraction pattern (diffraction position θ, diffraction intensity I). The diffraction patterns of multiple crystals in materials are superimposed without interference in the diffraction spectrum. The diffraction intensity of a crystal depends on its relative content in the material. According to Fig. 2d, the main minerals in loess are quartz, albite, calcite, illite and kaolinite. The minerals (inorganic substances) in the purchased biochar derived from apple trees and branches are mainly calcite, magnesium calcite and quartz (Kim et al. 2011; Al-Wabel et al. 2013). The XRD spectra of loess and BALs are almost identical possibly due to the same reason mentioned above; however, slight disparities in the intensities of specific crystals imply potential differences in their contents between loess and BALs.

3 Results and analysis

The SWRCs are presented in terms of gravimetric water content in this study. It is worth noting that the drying-induced volume change under null pressure condition is very small for both intact and compacted loess (Ng et al. 2016; Hou et al. 2020; Xiao et al. 2022). And biochar was reported to play a positive role in alleviating soil shrinkage and cracking (Lu et al. 2021; Puspanathan et al. 2022). For these reasons, the shrinkage of BAL during drying could also be too small to be considered, see Fig. 3.

3.1 SWRCs of the BAL specimens with different biochar contents

The SWRCs of the BAL specimens with different biochar contents, while the same molding water content and dry density, are summarized in Fig. 5. It is evident that the SWRCs of the biochar-amended specimens are consistently above those of the specimens without biochar, which indicates that the addition of biochar significantly improves the water retention capacity of compacted loess.

Firstly, the saturated water content of BAL increases with the increase of biochar content. For example, the saturated water contents of the BAL specimens (with a molding water content and dry density of 14% and 1.4 g/cm^3 respectively) are 32.6%, 36.5%, 36.9% and 37.9%, respectively, corresponding to the biochar contents of 0%, 5%, 10% and 20%, as shown in Fig. 5a. The saturated water content of the specimen with 10% biochar is a little less than that of the specimen with 5% biochar, as shown in Fig. 5b, which is probably because the former was not fully saturated (all specimens that achieved a degree of saturation not less than 95% were considered to have met the test standard). In summary, the addition of biochar can increase the saturated water content of compacted loess; the higher the biochar content, the larger the saturated water content of BAL. Similar results were obtained by Ouyang et al. (2013), Hardie et al. (2014) and Yi et al. (2020), who carried out investigations on sandy loams amended with biochar derived from various feedstocks (i.e., dairy manures pyrolyzed at 700 °C, acacia trees pyrolyzed at 550 °C, yellow pine pyrolyzed at 550 °C, and poultry litters pyrolyzed at 300 °C). Bordoloi et al. (2018) examined the water retention capacity of a sandy clay amended with water hyacinth biochar, and their results showed a positive relationship between the saturated water content and biochar content for biochar-amended sandy clay. Typically, the saturated water content of a soil specimen can be calculated from the specific gravity and known dry density, according to the mass-volume relationship of soil. According to $w_{sat} = 1/\rho_d - 1/G_s$, the saturated water content, w_{sat}, will decrease with

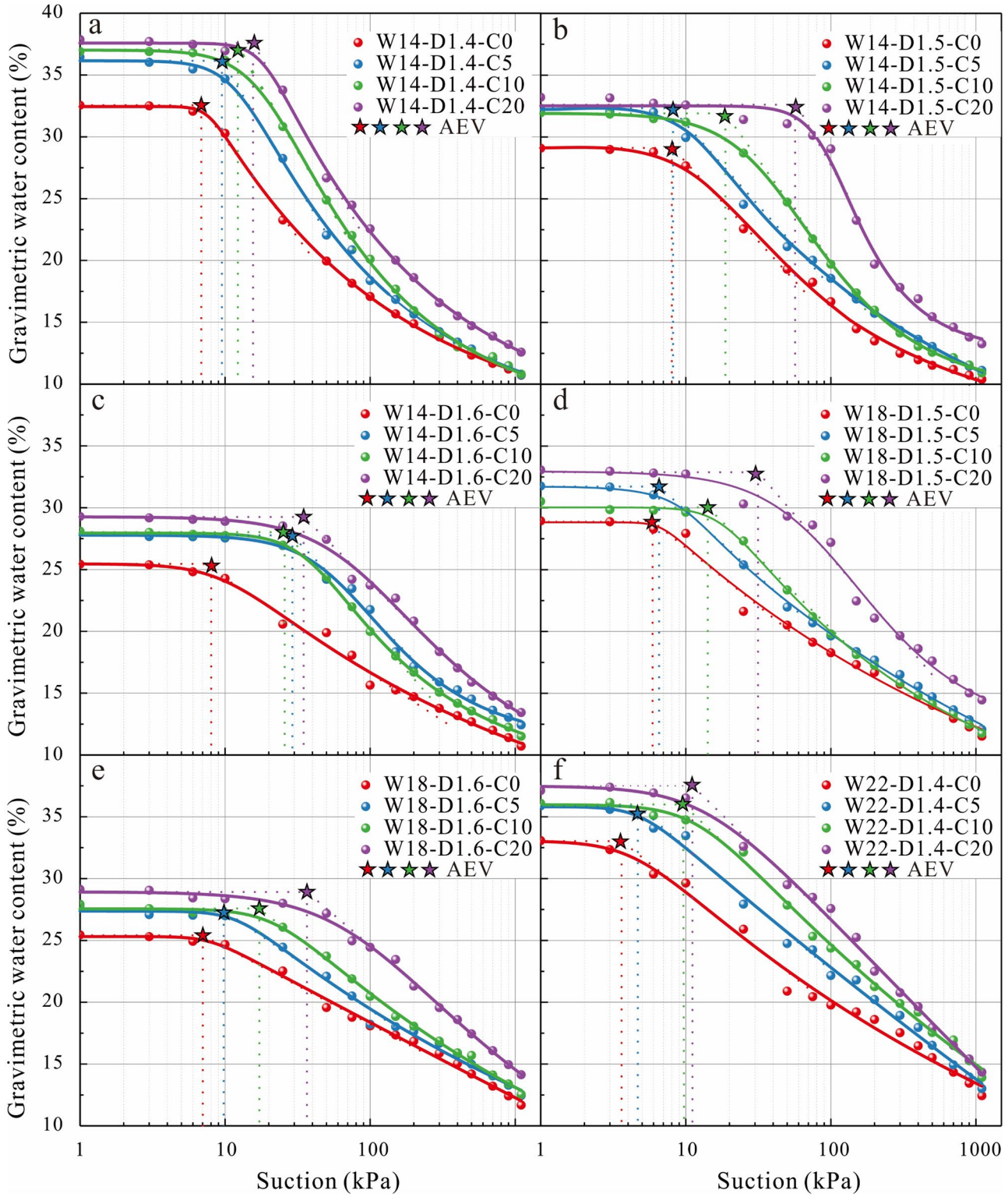

Fig. 5 SWRCs of the BAL specimens with different biochar contents (W denotes the molding water content, %; D denotes the dry density, g/cm^3; C denotes the biochar content, %; AEV is the air-entry value. With the increase of biochar content, the saturated water content increases, the AEV increases, and the desaturation rate slightly increases)

the increase of biochar content, which is obviously different from the measured data. This is because unlike soil particles, biochar particles are porous, and the mass-volume relationship of soil cannot be used to calculate the saturated water content of BAL.

Secondly, the AEV of BAL increases with the increase of biochar content. It is shown in Fig. 5a, at the biochar contents of 0%, 5%, 10% and 20%, the corresponding AEVs are 6.9 kPa, 9.4 kPa, 12.1 kPa and 15.4 kPa, respectively. That could be because the incorporation of biochar reduces the size of inter-aggregate pores in compacted specimen. The pore-size distribution curves (PSDs) of these specimens (which will be presented and elucidated in detail in the discussion) show that the dominant diameter of inter-aggregate pores in BAL decreases with the increase of biochar content. In the studies by Ouyang et al. (2013), Mollinedo et al. (2015), Rasa et al. (2018) and Hussain et al. (2020b), the SWRCs of various biochar-amended soils (sandy loam amended with animal manure biochar, corn straw biochar, and switchgrass biochar; silty sand amended with water hyacinth biochar and mesquite biochar; silty clay amended with animal manure biochar; clay amended with willow biochar) were compared with those of untreated soils. And it was found that the addition of biochar increased the AEV of soil. In addition, Chen et al. (2022b) measured the SWRCs of a silty sand amended with peanut shell biochar at varying contents (i.e., 0%, 10% and 20%) during drying and wetting processes. The results suggested that both the AEV and air-occlusion value (AOV) of biochar-amended silty sand were increased in response to an increase in biochar content. However, Wong et al. (2022) determined the SWRC of a kaolin amended with peanut shell biochar through the column test (i.e., transient profile method), and found that the influence of biochar on the AEV was not clear. A study by Chen et al. (2022a) on a loess amended with coconut shell biochar showed that the addition of biochar reduced the AEV of loess, which differs from the results of this study and may be attributed to variations in the type or wettability of biochar (hydrophilic or hydrophobic).

Finally, the addition of biochar affects the slope of the SWRC in the transition zone; with the increase of biochar content, the slope of the curve in the transition zone slightly increases. That is, the desaturation rate of loess is raised, because soil desaturation mainly occurs in the transition zone (Fredlund et al. 2012). As depicted in Fig. 5, the SWRC of BAL gradually becomes steeper as the biochar content increases from 0 to 20%. This is consistent with the observation of Lei and Zhang (2013), Andrenelli et al. (2016) and Alghamdi et al. (2020), which can also be attributed to the porosity of biochar. It can be observed from the micrographs (Fig. 4) that the size of intra-particle pores of biochar is a few microns to dozens of microns, which is close to the size of inter-aggregate pores in compacted loess (Xiao et al. 2022; Li et al. 2023). Therefore, in the transition zone (the stage at which inter-aggregate pores desaturate), water retained in biochar pores is discharged due to suction increase. In response to the same suction increase, the larger the content of biochar, the larger the amount of water drained from BAL and the higher the desaturation rate.

3.2 SWRCs of the BAL specimens with different molding water contents or dry densities

The SWRCs of the compacted specimens with different dry densities (1.4 g/cm^3, 1.5 g/cm^3 and 1.6 g/cm^3), while the same molding water content and biochar content, are summarized in Fig. 6. It can be seen that at the same molding water content and biochar content, the influence of dry density is mainly on the saturated water content and AEV; the larger the dry density of specimen, the smaller the saturated water content and the larger the AEV. This is in line with the mainstream view since particles are packed more closely with the increase in dry density (Xiao et al. 2022; Xu et al. 2023a, b). For example, similar findings were reported by Jiang et al. (2017) and Hou et al. (2020) for compacted sandy loess, and by Xiao et al. (2022) for compacted clayey loess. However, Wong et al. (2017) reported that the saturated water content increased in response to the increase in compaction degree for biochar-amended kaolin. Moreover, the addition of biochar intensifies the impact of dry density on the AEV. For example, the AEVs of the compacted specimens without biochar with the dry densities of 1.4, 1.5 and 1.6 g/cm^3 are 6.1 kPa, 6.8 kPa, and 7.9 kPa, respectively, as depicted in Fig. 6a. After the addition of biochar, the difference in AEV resulting from the variation of dry density increases. The AEVs of the specimens with 10% biochar are 6 kPa, 12 kPa and 18 kPa, respectively, corresponding to the dry densities of 1.4, 1.5 and 1.6 g/cm^3 (Fig. 6c); the AEVs are 12 kPa, 28 kPa and 34 kPa, respectively, when 20% biochar was added (Fig. 6d). In addition, a study by Xiao et al. (2022) presented that the SWRCs in terms of gravimetric water content of compacted loess specimens with different dry densities were basically coincident when suction was greater than 30 kPa. That is to say, dry density had little influence on the dehydration of compacted loess when suction was greater than 30 kPa. It is shown in Fig. 6, at the same molding water content and biochar content, the SWRCs of the compacted specimens with different dry densities also tend to coincide. In other words, as suction increases, the impact of dry density on the water retention capacity of BAL weakens and may disappear as suction reaches a critical value. This critical suction for BAL seems larger than that of the specimens without biochar. For example, this suction for the specimens with a low biochar content (e.g., 0%, 5%) is about 100 kPa (Fig. 6a, b), and exceeds 100 kPa for the specimens with a high biochar

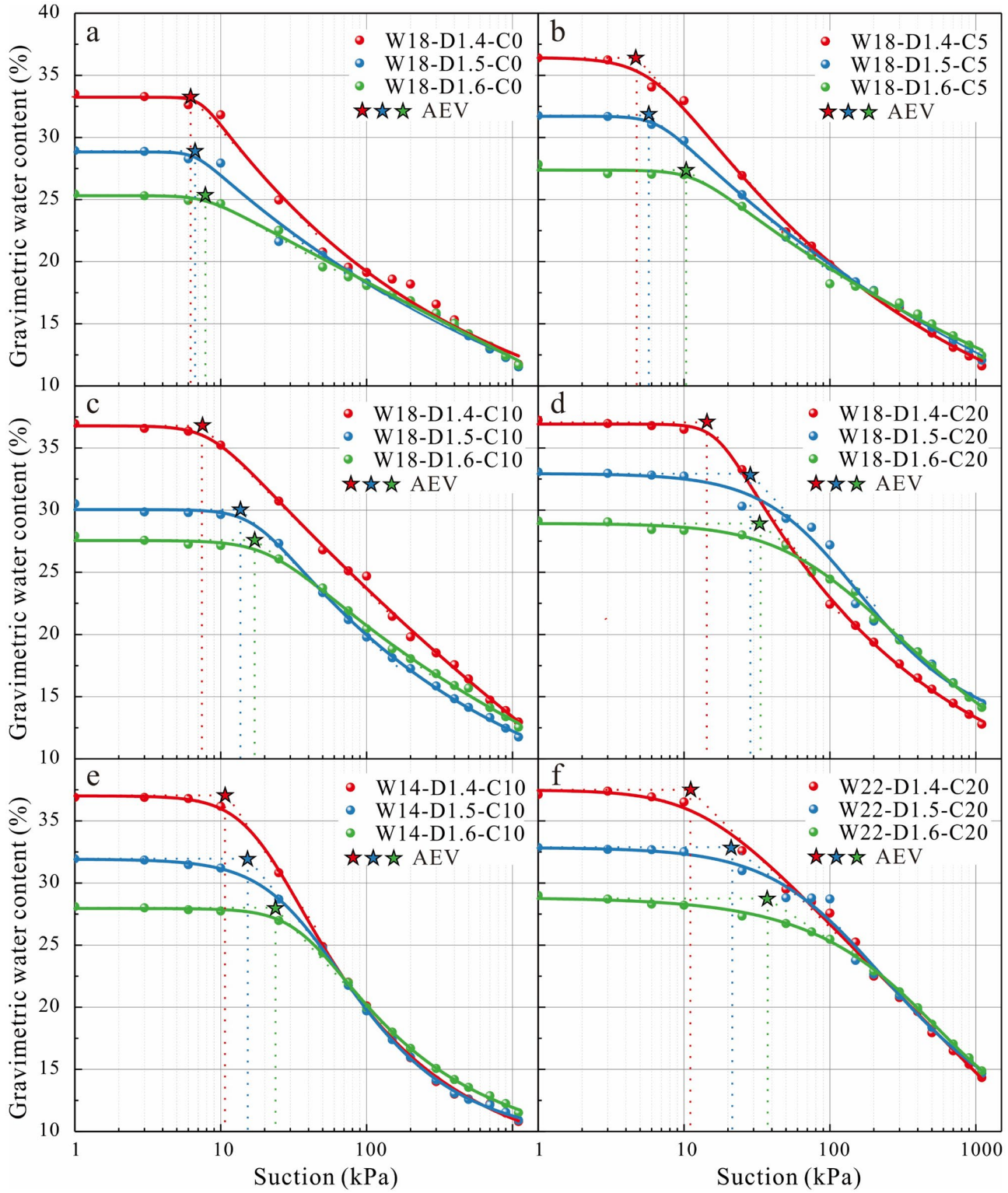

Fig. 6 SWRCs of the BAL specimens with different dry densities (W denotes the molding water content, %; D denotes the dry density, g/cm^3; C denotes the biochar content, %; AEV is the air-entry value. The influence of dry density is mainly on the saturated water content and AEV, and the addition of biochar intensifies the impact of dry density on the AEV)

content (e.g., 20%) (Fig. 6f). In Figs. 6c, d, this suction may be much greater because there remain obvious differences among the curves within the range of measurement (0–1000 kPa). A study by Wong et al. (2017) on peanut shell biochar-amended kaolin also showed that the difference in water content was less than 1% among the specimens with different dry densities in the high suction range (48.49–124.56 MPa).

Figure 7 displays the SWRCs of the compacted specimens with different molding water contents, while the same dry density and biochar content. The results of Xiao et al. (2022) indicate that different molding water contents can result in different AEVs and desaturation rates for compacted loess, specifically, the AEV and slope in the transition zone decrease with the increase of molding water content. They interpreted that molding water content has a control on the size of particles or aggregates in compacted loess, thus controlling the size of inter-aggregate pores. The specimen molded at a higher water content has smaller aggregates, as well as smaller inter-aggregate pores, in comparison to the specimen molded at a lower water content. In consequence, the former specimen has a lower rate of desaturation, or a flatter slope in the transition zone, and a higher AEV, than the latter. It is shown in Fig. 6, molding water content has a similar influence on the SWRC of BAL; that is, at a given dry density, the AEV of BAL decreases a little with an increase in molding water content. For instance, as molding water content increases from 14 to 22%, the AEV of BAL with 10% biochar decreases from 23.5 kPa to 14.2 kPa at the dry density of 1.6 g/cm^3 (Fig. 6c); the AEV of BAL with 20% biochar decreases from 33.0 kPa to 20.8 kPa (Fig. 6f). With an increase in molding water content, the slope of the SWRC in the transition zone decreases, meaning that the desaturation of BAL slows down. It should be noted that for the compacted specimens with the same dry density and biochar content, their SWRCs intersect at a suction between 20 and 50 kPa in the transition section. Molding water content has an impact on the SWRC of BAL, which is essentially on the PSD of BAL (Xiao et al. 2022).

4 Discussion

According to the results summarized above, the biochar-induced modifications of the SWRC of compacted loess are mainly on the saturated water content, AEV and desaturation rate. The direct influence of biochar on the water retention behavior of compacted loess mainly comes from two aspects. On the one hand, the physicochemical properties of biochar differ from those of loess, including the organic matter content and surface properties (i.e., surface charges and functional groups). On the other hand, biochar particles have a porous structure. Both can directly result in differences in the structure, physical, hydraulic and mechanical properties between BAL and natural loess (compacted loess). The indirect influence of biochar is that it might promote the microbial biomass, activity and diversity in soil as a carbon source. This may lead to the occurrence of bio-cementations (organic binding agents) and biological voids in soil, thereby resulting in changes in the soil structure and mechanical properties (Palansooriya et al. 2019; Kocsis et al. 2022). However, the indirect effect of biochar may only be evident under appropriate environmental conditions, such as humidity, temperature, oxygen level, pH and so on. Therefore, this study focuses on discussing the direct effects induced by the above two aspects, and the indirect effects of biochar are not considered.

4.1 Influence of biochar on the wettability of loess

Biochar is composed of organic matter or organic carbon (aromatic carbon, aliphatic carbon, etc.) and inorganic matter or ash (mainly refer to minerals, such as carbonates and phosphates, etc.) (Xu et al. 2017). The apple tree biochar used in the present study was found to contain about 47% organic carbon (Li et al. 2020a). The physicochemical properties of biochar are controlled by the organic matter it contains (Lee et al. 2010; Xu et al. 2017). The functional groups, refer to atoms or atomic groups that have a control on the physicochemical properties of organic compounds, thus govern the properties of biochar. The functional groups may be hydrophilic or hydrophobic. For example, oxygen-containing functional groups (e.g., carboxyl, hydroxyl, and aldehyde groups) have a similar structure to water molecules (charge polarity) and are capable of forming hydrogen bonds with them (Vander Spoel et al. 2006; Das and Sarmah 2015; Suliman et al. 2017). However, aliphatic functional groups (e.g., -CH) and aromatic functional groups (e.g., C–C) are nonpolar in structure, and thus hydrophobic (Fan et al. 2022). The type and quantity of functional groups on the surfaces of biochar particles determine its wettability. From the FTIR spectrums (Fig. 2c), the surface functional groups of apple tree biochar are mainly phenolic hydroxyl groups (-OH) and carbonyl groups (C=O), which are hydrophilic functional groups. This explains why the measured contact angles of biochar and BALs are less than 90°, as shown in Fig. 2b. Both the loess and biochar studied are hydrophilic, and the biochar is more hydrophilic since its initial contact angle is close to zero; the addition of biochar enhances the hydrophilicity of loess, i.e., the contact angle of BAL reduces more dramatically with an increase in biochar content. Suliman et al. (2017) once investigated the correlation between the water retention capacity of biochar-amended soil and the presence of oxygen-containing functional groups in biochar. They found that after the oxidation treatment (heating biochar in air at 250 °C), oxygen-containing functional groups (such as carboxyl, phenolic hydroxyl,

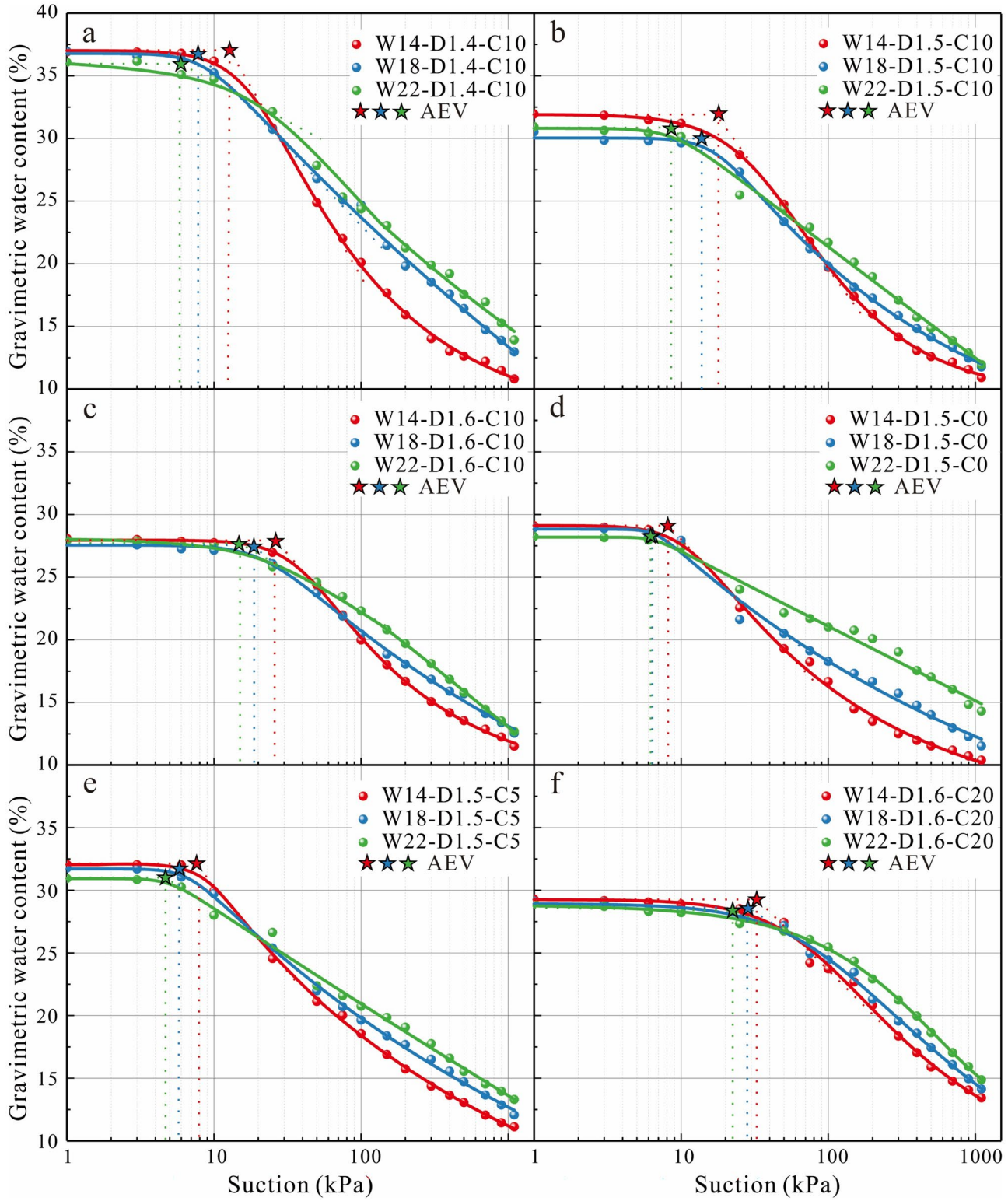

Fig. 7 SWRCs of the BAL specimens with different molding water contents (W denotes the molding water content, %; D denotes the dry density, g/cm^3; C denotes the biochar content, %; AEV is the air-entry value. With an increase in molding water content, the AEV of BAL decreases a little and the desaturation in the transition zone slows down)

and carbonyl groups) on the surfaces of biochar could reach 75.34% of the total amount of functional groups. The hydrophilicity of biochar was enhanced, and the water retention capacity of sand amended with oxidized biochar was significantly improved compared to that of sand amended with unoxidized biochar. In addition, the influence of biochar is associated with the organic matter content and hydrophilicity of soil. For example, Mao et al. (2019) compared the water retention capacities of black soil, loess and red soil amended with plant tissue biochar and dairy manure biochar with that of their duplicates without biochar. The addition of biochar (both plant tissue biochar and dairy manure biochar) was found to only improve the water retention capacity of loess and red soil, which have a low organic carbon content and are hydrophilic, while had little impact on the water retention capacity of black soil which has a high organic carbon content and is hydrophobic.

The surfaces of biochar particles could be both negatively charged and positively charged due to the dissociation and protonation of functional groups, with the quantity of charges depending on the environmental pH. As per He et al. (2022), the pH_{pzc} (the pH at the point of zero charge, positive and negative charges are balanced) of apple tree biochar is about 3.3. This means when the environmental pH exceeds 3.3, the dissociation of functional groups is dominated, and the particles of apple tree biochar are thus negatively charged. Generally, a greater difference between the environmental pH and pH_{pzc} leads to a higher degree of dissociation of functional groups, as well as a larger density of negative charges on the biochar particle surfaces. Under normal conditions, apple tree biochar is negatively charged in loess, which is attributed not only to the pH of loess (varies between 7.0 and 8.1, according to He et al. 2022), but also to the pH of apple tree biochar (9.52, see Table 2; as per Zhao et al. 2015; Tan et al. 2020). Both pHs are much higher than the pH_{pzc} of apple tree biochar, suggesting that the surface functional groups of biochar are highly dissociated. Biochar particles possess abundant negative charges on their surfaces, which attract water molecules by electrostatic attraction, like clay particles. Therefore, the water retention capacity of compacted loess is improved as a result of the addition of apple tree biochar.

4.2 Influence of biochar on the structure of compacted loess

On the one hand, unlike soil particles, biochar particles are porous. Apple tree (*pumila Mill*) is a vascular plant, like most terrestrial plants such as trees, shrubs and herbs. Water and nutrients transport from roots to other parts of the plant, such as stems and leaves, through the vascular system that is composed of xylem and phloem. Such a structure benefits the long-distance transport of fluids in the plant (Lucas et al. 2013), and could be preserved during pyrolysis (see Fig. 4). Numerous tubular pores with diameters exceeding 10 μm have been observed in other wood-based biochar (e.g., Lin et al. 2012; Hyväluoma et al. 2018). Sun and Lu (2014) measured the PSDs of straw biochar and woodchip biochar using MIP and suggested that around 35% of the total porosity of straw biochar is contributed by the pores with entrance diameters > 75 μm, followed by the 0.1 – 5 μm class (≈ 25%), and the 5 – 30 μm class (≈ 22%), while the PSD of woodchip biochar appeared to be bimodal with two peaks at 4 – 5 μm and around 8 μm (see Fig. 8a). Rasa et al. (2018) and Turunen et al. (2020) characterized the pore structure of biochar particle derived from various plant biomass (e.g., willow, hemp hurd, and mixed wood) using micro-CT, and quantified the morphological characteristics of intra-particle pores of biochar by image processing. They found that the diameters of intra-particle pores of all three biochars were concentrated in the range of 2–12 μm, with a dominant diameter close to 7–9 μm (as shown in Fig. 8a). The discrepancy between the results of MIP and micro-CT mainly stems from the limitations of each technique. Specifically, MIP quantifies the PSD of a compacted biochar specimen (a number of stacked biochar particles, > 1 cm^3 in volume), thus, it is likely that the large pores (> 20 μm pores) are pores between biochar particles rather than intra-particle pores. In contrast, micro-CT is limited by the image resolution although all the pores detected are intra-aggregate pores, those with sizes smaller than the image resolution (0.568 μm in their studies) cannot be identified currently. Moreover, the pore diameter determined by micro-CT refers to the equivalent sphere diameter, which is the diameter of an equivalent sphere with the same volume as that of the three-dimensional pore. Whereas, MIP assumes that the three-dimensional pore is cylindrical and determines its diameter (i.e., the entrance diameter) following the Laplace's capillary law. Therefore, both diameters cannot accurately represent the size of a three-dimensional pore, which is also variable due to the irregular shape of pores in natural materials. The combined use of these two techniques may lead to a more accurate understanding of the size distribution of intra-particle pores of biochar. In the present study, we also measured the PSD of apple tree biochar using MIP, as shown in Fig. 8b. The large pores (> 20 μm diameter) are probably inter-particle pores resulting from particle arrangement, whereas it can be confirmed that the size of intra-particle pores of biochar mainly falls in the range of 0.5–10 μm. The pores in BAL were categorized into three groups based on the MIP-determined pore diameter, and the volume ratio of each group was calculated and summarized in Fig. 8d. The addition of biochar is demonstrated to increase the pore density within the range of 0.5 – 10 μm, which further increases with an increase in biochar content, i.e., 33.8%, 50.9%, 55.39% and 65.36% corresponding to the biochar

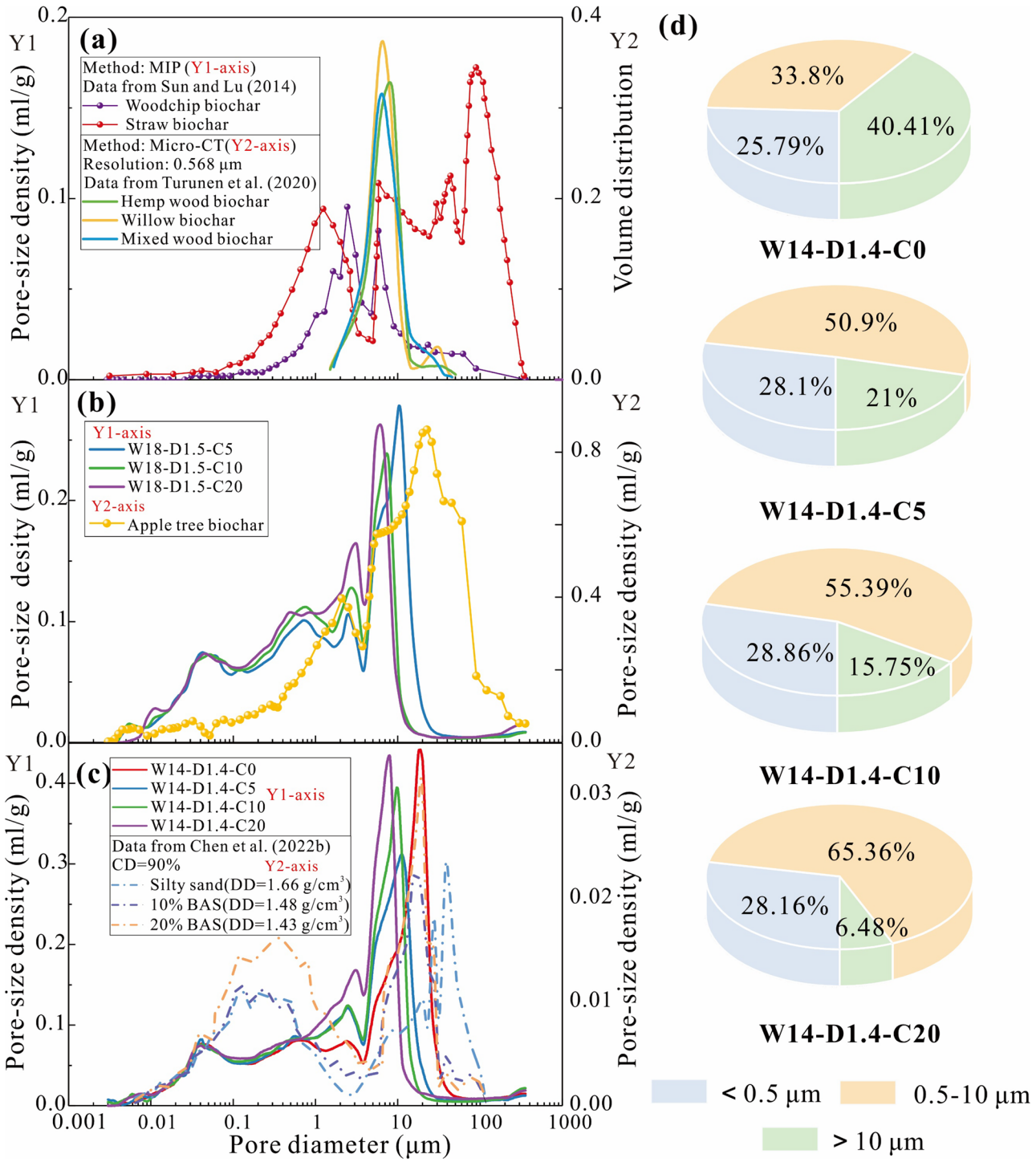

Fig. 8 **a**–**c** PSDs of various biochar and BAS specimens; **d** volume ratios of different pore groups in BAL specimens (CD means the compaction degree, BAS is short for biochar-amended soil)

contents of 0%, 5%, 10% and 20%, respectively. Therefore, apple tree biochar particles are porous and have good pore connectivity (Rasa et al. 2018; Lu and Zong 2018). Such a structure allows biochar particles to store or drain water. In compacted loess, the diameter delimiting inter-aggregate and intra-aggregate pores varies with the grain-size distribution (GSD) and method used to determine the PSD, and ranges between 0.1 and 3 μm (Ng et al. 2016; Li et al. 2020b; Xiao et al. 2022). In that case, most intra-particle pores of biochar have sizes larger than the delimiting diameter of compacted

loess, suggesting that these pores may belong to the family of inter-aggregate pores in BAL. In other words, the incorporation of biochar could potentially alter the PSD of inter-aggregate pores of compacted loess. This is evidenced by the PSDs of the BAL specimens, as shown in Figs. 8b, c. That is to say, the volume of inter-aggregate pores is increased due to the biochar addition, thereby leading to significant modifications to the soil water retention and drainage behavior (Fig. 5). In summary, wood-based biochar particles are porous in nature, with vascular bundles featuring large sizes ranging from 0.5 to 10 μm. The addition of biochar greatly changes the PSD, resulting in an increase in the density or volume of large pores (inter-aggregate pores), thereby enhancing the soil water retention capacity (saturated water content) and drainage capacity (rate of desaturation in the transition zone) (Sun and Lu 2014; Liu et al. 2016).

It should be stated that some intra-particle pores of biochar (with large sizes) may be filled with fine soil particles when fully mixed and compacted (Wong et al. 2017; Vijayaraghavan 2021; Liu et al. 2022). If the biochar pores are mostly filled with fine soil particles, the impact of biochar's macroporosity on the soil PSD and SWRC may be diminished due to the reduced pore connectivity. However, under such a condition, the density increase in BAL may not fall in the range of 0.5–10 μm (the size range of biochar pores), which deviates from the experimental finding. For this reason, the biochar pores were not be fully filled with soil particles. The micrographs also reveal that the biochar pores were partially filled with a small number of fine particles (Fig. 4d); the PSDs indicate that the most significant increase in the pore-size density occurs within 0.5–10 μm in the BAL specimens (Figs. 8b, c), by around 20–32% (Fig. 8d), and the pores smaller than this range are largely unaffected (by around 2%) (Fig. 8d). In summary, the porous structure of apple tree biochar provides more water retention spaces and drainage channels in amended loess compared to natural loess. Therefore, under any suction, the water contents of the BAL specimens are higher than those of untreated loess specimens, and the drainage rates in the transition stage of the BAL specimens are larger than those of untreated loess specimens.

On the other hand, the addition of biochar changes the type and size of aggregates in compacted loess, which in turn affects the pore structure of compacted loess. As mentioned above, oxygen-containing functional groups on the surfaces of biochar particles can provide or accept hydrogen ions for the formation of hydrogen bonds; so, biochar particles may attract clay particles through hydrogen bonds and electrostatic attraction. It can be observed from Fig. 9a, b that a substantial quantity of clay particles is adsorbed onto the surfaces of biochar particles. Meanwhile, there is a large quantity of anionic charges on the surfaces of biochar particles, which enables them to adsorb cations and water molecules. For these reasons, organic-inorganic complexes could be formed via cationic bridging or through the sharing of bound water films (Fig. 9a, b). Some scholars have discussed the interaction between biochar particles and soil minerals. For example, Keiluweit and Kleber (2009) and Joseph et al. (2010) proposed that the interaction between biochar particles and clay minerals is similar to that between organic matter and clay minerals, and the main inter-particle forces are van der Waals attraction, hydrogen bonding, electrostatic attraction, and cation bridging, e.g., Fe^{3+}, Al^{2+}. These forces are related to the type of clay mineral and surface properties of biochar (e.g., type and quantity of functional groups) (Yang et al. 2016). In a word, biochar and mineral particles can form organic-inorganic complexes through van der Waals attraction, electrostatic attraction, cation bridging and hydrogen bonding; these complexes serve as an important type of aggregate in biochar-amended soil (Kleber et al. 2007; Keiluweit and Kleber 2009; Joseph et al. 2010). From Fig. 9c, e, we can clearly see that most aggregates in untreated loess specimens are silt aggregates, while the BAL specimens contain many complexes formed by clays wrapping biochar particles (Fig. 9d, f). That is to say, aggregate remains the fundamental element of the BAL structure, while the type of aggregate differs from that in compacted loess. Moreover, BAL and untreated loess have different sizes of aggregates. In comparison to untreated loess, the sizes of silt and clay aggregates in BAL are smaller, while the size of organic-inorganic complexes is much larger, see Fig. 9e, f. This is because the addition of biochar affects the occurrence of clay particles and hinders the formation of silt aggregates. In this case, aggregates with a wide range of sizes are arranged more closely in BAL. This explains the test results that there are fewer large pores (i.e., > 20 μm) in the BAL specimens compared to the specimen without biochar, despite having the same dry density (see Fig. 8c).

4.3 Significance, limitations and future perspectives

The present study investigated the water retention behavior of BAL in order to explore its potential applications in geotechnical or geo-environmental engineering in loess regions, the main contributions and innovations can be summarized into two aspects. 1) This study aimed at compacted BAL with high degrees of compaction since engineered slopes, embankments, and landfill covers often require high compaction conditions. This could fill a knowledge gap in current research that studies on densely compacted BAL are quite lacking, and most related studies aimed at the nutrient availability, water availability, plant growth, soil tillability and soil remediation (Han et al. 2016; Su et al. 2019; Luo et al. 2020). However, biochar has been recognized as a promising soil amendment for enhancing soil properties

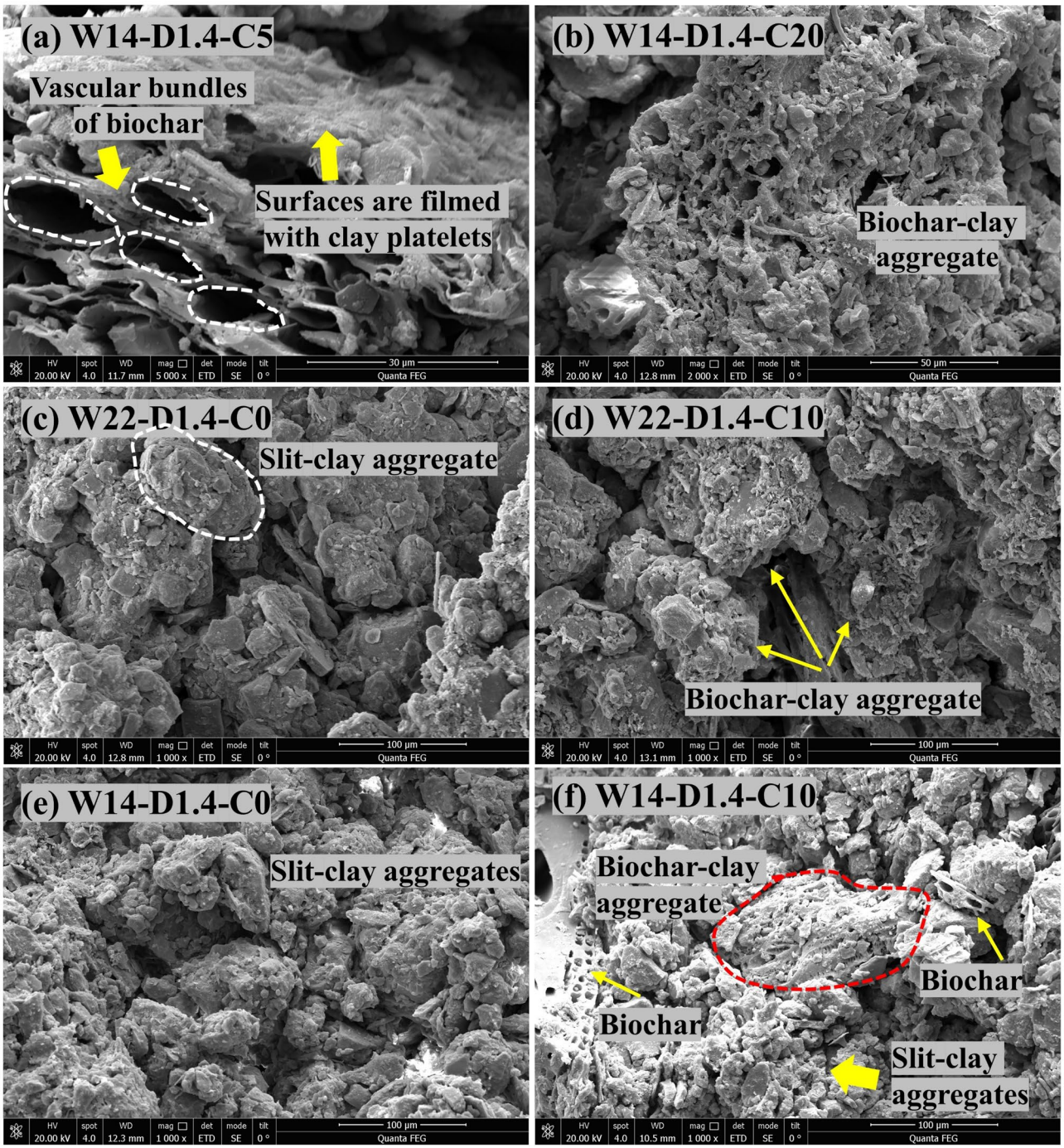

Fig. 9 Micrographs of the BAL specimens

such as alleviating cracking and retaining water. And it is currently used in man-made earth structures where the soils, unlike loose planting soils, are typically compacted to high degrees of compaction (Wong et al. 2017; Ng et al. 2022; Guo et al. 2023). Additionally, the SWRCs of BALs with various biochar contents were examined over a wide range of suction, as engineered soils may experience extreme droughts and produce high suctions in practice. 2) This study presents a comprehensive analysis of the underlying mechanisms by which biochar influences the SWRC of compacted loess by altering its surface properties and structure. The fundamental data and detailed interpretations presented can help fully understand how specific properties of biochar can have a control over the water retention capacity of BAL,

as both biochar- and soil-related factors can influence the properties of biochar-amended soil.

However, our study also has limitations. 1) The shrinkage of compacted BAL during drying for measuring the SWRC was not considered in this study. 2) The suction range is not wide enough as it can be seen from Figs. 5, 6 and 7 that the boundary effect zone and transition zone of BALs during the desaturation were only concerned. Due to these limitations and knowledge gaps in research on biochar applications in geotechnical or geo-environmental engineering in loess regions, several perspectives could be proposed for our future research. First of all, further investigation could be conducted on the effects of biochar derived from different types of feedstocks, such as woodchips, crop residues, animal manures, sewage sludges, grasses and biosolids, as feedstock and pyrolysis process have a significant impact on the physicochemical properties of biochar. Then, more hydraulic and mechanical properties of compacted BAL with high degrees of compaction could be examined, such as permeability, compressibility, shear strength, tensile strength, and volume change behavior, since they are important for evaluating engineered soils. Actually, we also performed some mechanical tests on compacted BALs (with different compaction degrees, biochar contents, etc.), such as triaxial tests, unconfined compression tests, and infiltrations tests, which will be presented and discussed in another paper due to the space limitation. Moreover, it is imperative to conduct more comprehensive and rigorous experimental investigations on the water retention behavior of compacted BAL. Specifically, careful consideration should be given to the volume change during drying or wetting of compacted BAL, and further examination of its SWRC over a wider range of suction is warranted. And constitutive equations for modelling the SWRC of compacted BAL could be proposed, which can take into account the biochar-induced modifications to the soil hydrophilicity and pore structure. Last but not least, investigations on the long-term effects of biochar are imperative since biochar, as a carbon source, will inevitably interact with soil microorganisms (microbial decomposition) and plants, even if it is wrapped with fine particles in soil. In that case, the temporal variation of biochar influence holds great significance for geotechnical or geo-environmental applications. In addition, revealing the potential environmental implications associated with the applications of biochar in geotechnical or geo-environmental engineering is of importance.

5 Conclusions

In this study, the influence of biochar on the water retention behavior of loess was investigated and a comprehensive and detailed analysis of the underlying mechanisms was provided. Additionally, several perspectives were proposed for future research. Several important conclusions can be drawn.

The addition of biochar significantly improves the water retention capacity of compacted loess. With the increase of biochar content, the saturated water content increases, the AEV increases, and the desaturation rate slightly increases. The influence of dry density is mainly on the saturated water content and AEV, and the addition of biochar intensifies the impact of dry density on the AEV. The influence of molding water content on the SWRC of BAL is similar to that on the SWRC of compacted loess.

The effects of biochar can primarily be attributed to the modifications induced by biochar on the physicochemical properties and structure of loess. On the one hand, the apple tress biochar studied is highly hydrophilic due to the presence of abundant oxygen-containing functional groups and negative charges on its surfaces, thus significantly enhancing the soil wettability. On the other hand, the biochar addition increases the volume of inter-aggregate pores and changes the type and size of aggregates, aggregates with a wide range of sizes are arranged more closely in BAL, therefore, the soil water retention capacity and drainage capacity are improved.

This study provides a theoretical basis for the applications of biochar in geotechnical or geo-environmental engineering in loess regions, however, further investigations are imperative, including: 1) examining the effects of biochar derived from various types of feedstocks on loess; 2) investigating the hydraulic and mechanical properties of BAL under high compaction conditions; 3) studying the water retention behavior of compacted BAL in depth; 4) exploring the temporal variation of the biochar influence.

Supplementary Information The online version contains supplementary material available at https://doi.org/10.1007/s11368-023-03701-w.

Acknowledgements Additional thank is given to Dr. Xiao Tao and six anonymous Reviewers for their valuable comments and suggestions.

Credit authorship contribution statement Liang Sun: Investigation, figure preparation, and manuscript writing. Ping Li: Idea proposing, analyzing, manuscript writing & revision, supervision. Wenbin Fei: Revision, discussion. Jiading Wang: Supervision.

Funding This work was funded by the National Natural Science Foundation of China (42007251, 42027806).

Data availability The data that support the findings of this study are available from the corresponding author, PL, upon reasonable request.

Declarations

Competing interest The authors declare that they have no competing financial interests or personal relationships that could have appeared to influence the work reported in this paper.

References

Abel S, Peters A, Trinks S, Schonsky H, Facklam M, Wessolek G (2013) Impact of biochar and hydrochar addition on water retention and water repellency of sandy soil. Geoderma 202:183–191

Al-Wabel MI, Al-Omran E, El-Naggar AH, Nadeem M, Usman ARA (2013) Pyrolysis temperature induced changes in characteristic and chemical composition of biochar produced from conocarpus wastes. Bioresource Technol 131:374–379

Alghamdi AG, Alkhasha A, Ibrahim HM (2020) Effect of biochar particle size on water retention and availability in a sandy loam soil. J Saudi Chem Soc 24(12):1042–1050

Anand A, Kumar V, Kaushal P (2022) Biochar and its twin benefits: Crop residue management and climate change mitigation in India. Renew Sust Energ Rev 156:111959

Andrenelli MC, Maienza A, Genesio L, Miglietta F, Pellegrini S, Vaccari FP, Vignozzi N (2016) Field application of pelletized biochar: short term effect on the hydrological properties of a silty clay loam soil. Agr Water Manage 163:190–196

ASTM D698-12 (2012) Standard test methods for laboratory compaction characteristics of soil using standard effort. Annu B ASTM Stand

ASTM (2013) Annual book of ASTM standards. ASTM International, West Conshohocken, Pa

Bansal RC, Donnet JB, Stoeckli F (1988) Active Carbon. Marcel Decker. Inc., New York, p 482

Bordoloi S, Garg A, Sreedeep S, Lin P, Mei G (2018) Investigation of cracking and water availability of soil-biochar composite synthesized from invasive weed water hyacinth. Bioresource Technol 263:665–677

Castellini M, Giglio L, Niedda M, Palumbo AD, Ventrella D (2015) Impact of biochar addition on the physical and hydraulic properties of a clay soil. Soil till Res 154:1–13

Chen W, Meng J, Han X, Lan Y, Zhang W (2019) Past, present, and future of biochar. Biochar 1:75–87

Chen X, Duan M, Zhou B, Cui L (2022a) Effects of biochar nanoparticles as a soil amendment on the structure and hydraulic characteristics of a sandy loam soil. Soil Use Manage 38(1):836–849

Chen XW, Wong JTF, Ng CWW, Wong MH (2016) Feasibility of biochar application on a landfill final cover—a review on balancing ecology and shallow slope stability. Environ Sci Pollut R 23:7111–7125

Chen XW, Wong JTF, Chen ZT, Tang TWL, Guo HW, Leung AOW et al (2018) Effects of biochar on the ecological performance of a subtropical landfill. Sci Total Environ 644:963–975

Chen Z, Kamchoom V, Apriyono A, Chen R, Chen C (2022b) Laboratory study of water infiltration and evaporation in biochar-amended landfill covers under extreme climate. Waste Manage 153:323–334

China Statistical Yearbook (2020) National Bureau of Statistics of China Online Database. http://www.stats.gov.cn/tjsj/ndsj/2020/indexch.htm

Chintala R, Mollinedo J, Schumacher TE, Malo DD, Julson JL (2014) Effect of biochar on chemical properties of acidic soil. Arch Agron Soil Sci 60(3):393–404

Das O, Sarmah AK (2015) The love–hate relationship of pyrolysis biochar and water: a perspective. Sci Total Environ 512:682–685

Edeh IG, Mašek O, Buss W (2020) A meta-analysis on biochar's effects on soil water properties–New insights and future research challenges. Sci Total Environ 714:136857

Fan M, Li C, Shao Y, Zhang S, Gholizadeh M, Hu X (2022) Pyrolysis of cellulose: Correlation of hydrophilicity with evolution of functionality of biochar. Sci Total Environ 825:153959

Fredlund DG, Rahardjo H, Fredlund MD (2012) Unsaturated soil mechanics in engineering practice. John Wiley Sons. Hoboken, United States

Garg A, Huang H, Cai WL, Reddy NG, Chen PN, Han YF, Kamchoom V, Gaurav S, Zhu HH (2021) Influence of soil density on gas permeability and water retention in soils amended with in-house produced biochar. J Rock Mech Geotech 13(3):593–602

Gluba Ł, Rafalska-Przysucha A, Szewczak K, Łukowski M, Szlązak R, Vitková J, Kobyłecki R et al (2021) Effect of fine size-fractionated sunflower husk biochar on water retention properties of arable sandy soil. Materials 14(6):1335

Gul S, Whalen JK, Thomas BW, Sachdeva V, Deng H (2015) Physico-chemical properties and microbial responses in biochar-amended soils: mechanisms and future directions. Agr Ecosyst Environ 206:46–59

Guo H, Zhang Q, Chen Y, Lu H (2023) Effects of biochar on plant growth and hydro-chemical properties of recycled concrete aggregate. Sci Total Environ 882:163557

Han F, Ren L, Zhang XC (2016) Effect of biochar on the soil nutrients about different grasslands in the Loess Plateau. Catena 137:554–562

Han JL, Zhang AF, Kang YH, Han JQ, Yang B, Hussain Q, Wang XD, Zhang M, Khan MA (2022) Biochar promotes soil organic carbon sequestration and reduces net global warming potential in apple orchard: A two-year study in the Loess Plateau of China. Sci Total Environ 803:150035

Hardie M, Clothier B, Bound S, Oliver G, Close D (2014) Does biochar influence soil physical properties and soil water availability? Plant Soil 376:347–361

He Z, Cao H, Liang J, Hu Q, Zhang Y, Nan X, Zhijun L (2022) Effects of biochar particle size on sorption and desorption behavior of NH4+-N. Ind Crop Prod 189:115837

Hewage SA, Roksana K, Tang CS, Zhuo Z, Zhu C (2023) Evaluation of cracking in biochar-amended clayey soil under freeze–thaw cycles. Transport Res Rec 2677(9):683–699

Hou X, Qi S, Li T, Guo S, Wang Y, Li Y, Zhang L (2020) Microstructure and soil-water retention behavior of compacted and intact silt loess. Eng Geol 277:105814

Huang H, Reddy NG, Huang XL, Chen PN, Wang PY, Zhang YT, Huang YX, Lin P, Garg A (2021) Effects of pyrolysis temperature, feedstock type and compaction on water retention of biochar amended soil. Sci Rep-UK 11(1):7419

Huovila A, Siikavirta H, Rozado CA, Rökman J, Tuominen P, Paiho S, Hedman Å, Ylén P (2022) Carbon-neutral cities: Critical review of theory and practice. J Clean Prod 341:130912

Hussain R, Bordoloi S, Gupta P, Garg A, Ravi K, Sreedeep S, Sahoo L (2020a) Effect of biochar type on infiltration, water retention and desiccation crack potential of a silty sand. Biochar 2:465–478

Hussain R, Ravi K (2022) Investigating biochar-amended soil as a potential lightweight material for embankments. Ecol Eng 180:106645

Hussain R, Ravi K, Garg A (2020b) Influence of biochar on the soil water retention characteristics (SWRC): Potential application in geotechnical engineering structures. Soil till Res 204:104713

Hyväluoma J, Kulju S, Hannula M, Wikberg H, Källi A, Rasa K (2018) Quantitative characterization of pore structure of several biochars with 3D imaging. Environ Sci Pollut R 25:25648–25658

IEA (2023) CO2 Emissions in 2022, IEA, Paris. https://www.iea.org/reports/co2-emissions-in-2022, License: CC BY 4.0

Igalavithana AD, Mandal S, Niazi NK, Vithanage M, Parikh SJ, Mukome FN et al (2017) Advances and future directions of biochar characterization methods and applications. Crit Rev Env Sci Tec 47(23):2275–2330

Ippolito JA, Cui L, Kammann C, Wrage-Mönnig N, Estavillo JM, Fuertes-Mendizabal T et al (2020) Feedstock choice, pyrolysis

temperature and type influence biochar characteristics: a comprehensive meta-data analysis review. Biochar 2:421–438
Jeffery S, Meinders MB, Stoof CR, Bezemer TM, van de Voorde TF, Mommer L, van Groenigen JW (2015) Biochar application does not improve the soil hydrological function of a sandy soil. Geoderma 251:47–54
Jiang Y, Chen W, Wang G, Sun G, Zhang F (2017) Influence of initial dry density and water content on the soil-water characteristic curve and suction stress of a reconstituted loess soil. B Eng Geol Environ 76:1085–1095
Joseph SD, Camps-Arbestain M, Lin Y, Munroe P, Chia CH, Hook J et al (2010) An investigation into the reactions of biochar in soil. Soil Res 48(7):501–515
Kameyama K, Miyamoto T, Iwata Y, Shiono T (2016) Effects of biochar produced from sugarcane bagasse at different pyrolysis temperatures on water retention of a calcaric dark red soil. Soil Sci 181(1):20–28
Keiluweit M, Kleber M (2009) Molecular-level interactions in soils and sediments: the role of aromatic π-systems. Environ Sci Technol 43(10):3421–3429
Kim P, Johnson A, Edmunds CW, Radosevich M, Vogt F, Rials TG, Labbé N (2011) Surface functionality and carbon structures in lignocellulosic-derived biochars produced by fast pyrolysis. Energy Fuels 25(10):4693–4703
Kleber M, Sollins P, Sutton R (2007) A conceptual model of organo-mineral interactions in soils: self-assembly of organic molecular fragments into zonal structures on mineral surfaces. Biogeochemistry 85:9–24
Kocsis T, Ringer M, Biró B (2022) Characteristics and applications of biochar in soil–plant systems: A short review of benefits and potential drawbacks. Appl Sci 12(8):4051
Lee JW, Kidder M, Evans BR, Paik S, Buchanan Iii AC, Garten CT, Brown RC (2010) Characterization of biochars produced from cornstovers for soil amendment. Environ Sci Technol 44(20):7970–7974
Lehmann J (2007) Bio-energy in the black. Front Ecol Environ 5(7):381–387
Lehmann J, Joseph S (Eds.) (2015) Biochar for environmental management: science, technology and implementation. Routledge
Lei O, Zhang R (2013) Effects of biochars derived from different feedstocks and pyrolysis temperatures on soil physical and hydraulic properties. J Soil Sediment 13:1561–1572
Li P, Li TL, Vanapalli SK (2018) Prediction of soil-water characteristic curve for Malan loess in Loess Plateau of China. J Cent South Univ 25(2):432–447
Li P, Pan Z, Xiao T, Wang J (2023) Effects of molding water content and compaction degree on the microstructure and permeability of compacted loess. Acta Geotech 18(2):921–936
Li P, Shao S, Vanapalli SK (2020a) Characterizing and modeling the pore-size distribution evolution of a compacted loess during consolidation and shearing. J Soil Sediment 20:2855–2867
Li YY, Feng G, Tewolde H, Yang M, Zhang F (2020b) Soil, biochar, and nitrogen loss to runoff from loess soil amended with biochar under simulated rainfall. J Hydrol 591:125318
Lian F, Huang F, Chen W, Xing B, Zhu LY (2011) Sorption of apolar and polar organic contaminants by waste tire rubber and its chars in single-and bi-solute systems. Environ Pollut 159(4):850–857
Lin Y, Munroe P, Joseph S, Henderson R, Ziolkowski A (2012) Water extractable organic carbon in untreated and chemical treated biochars. Chemosphere 87(2):151–157
Liu C, Wang HL, Tang XY, Guan Z, Reid BJ, Rajapaksha AU et al (2016) Biochar increased water holding capacity but accelerated organic carbon leaching from a sloping farmland soil in China. Environ Sci Pollut R 23:995–1006
Liu Z, Ogunmokun FA, Wallach R (2022) Does biochar affect soil wettability and flow pattern? Geoderma 417:115826
Lu S, Zong Y (2018) Pore structure and environmental serves of biochars derived from different feedstocks and pyrolysis conditions. Environ Sci Pollut R 25:30401–30409
Lu Y, Gu K, Shen Z, Tang CS, Shi B, Zhou Q (2023) Biochar implications for the engineering properties of soils: A review. Sci Total Environ 164185
Lu Y, Gu K, Zhang Y, Tang C, Shen Z, Shi B (2021) Impact of biochar on the desiccation cracking behavior of silty clay and its mechanisms. Sci Total Environ 794:148608
Lucas WJ, Groover A, Lichtenberger R, Furuta K, Yadav SR, Helariutta Y et al (2013) The plant vascular system: evolution, development and functions f. J Integr Plant Biol 55(4):294–388
Luo C, Yang J, Chen W, Han F (2020) Effect of biochar on soil properties on the Loess Plateau: Results from field experiments. Geoderma 369:114323
Mallapaty S (2020) How China could be carbon neutral by mid-century. Nature 586(7830):482–483
Mao J, Zhang K, Chen B (2019) Linking hydrophobicity of biochar to the water repellency and water holding capacity of biochar-amended soil. Environ Pollut 253:779–789
Mollinedo J, Schumacher TE, Chintala R (2015) Influence of feedstocks and pyrolysis on biochar's capacity to modify soil water retention characteristics. J Anal Appl Pyrol 114:100–108
Ng CWW, Sadeghi H, Hossen SB, Chiu CF, Alonso EE, Baghbanrezvan S (2016) Water retention and volumetric characteristics of intact and re-compacted loess. Can Geotech J 53(8):1258–1269
Ng CWW, Liao JX, Bordoloi S (2022) Relationship between matric suction and leaf indices of Schefflera arboricola in biochar amended soil. Canadian Geotech J 59(2):191–202
Ni JJ, Chen XW, Ng CWW, Guo HW (2018) Effects of biochar on water retention and matric suction of vegetated soil. Géotech Lett 8(2):124–129
Novak JM, Lima I, Xing B, Gaskin JW, Steiner C, Das KC, Ahmedna M, Rehrah D, Watts DW, Busscher WJ, Schomberg H (2009) Characterization of designer biochar produced at different temperatures and their effects on a loamy sand. Ann Environ Sci 3:195–206
Ouyang L, Wang F, Tang J, Yu L, Zhang R (2013) Effects of biochar amendment on soil aggregates and hydraulic properties. J Soil Sci Plant Nut 13(4):991–1002
Palansooriya KN, Wong JTF, Hashimoto Y, Huang L, Rinklebe J, Chang SX, Bolan N, Wang H, Ok YS (2019) Response of microbial communities to biochar-amended soils: a critical review. Biochar 1:3–22
Park SW, Kug JS (2022) A decline in atmospheric CO2 levels under negative emissions may enhance carbon retention in the terrestrial biosphere. Commun Earth Environ 3(1):289
Puspanathan TK, Jayawardane VS, Paul SC, Ying KS, Shukla SK, Anggraini V (2022) Effect of biochar on desiccation of marine soils under constant and cyclic temperatures. Acta Geotech 17(12):5441–5464
Rasa K, Heikkinen J, Hannula M, Arstila K, Kulju S, Hyväluoma J (2018) How and why does willow biochar increase a clay soil water retention capacity? Biomass Bioenerg 119:346–353
Reddy KR, Yaghoubi P, Yukselen-Aksoy Y (2015) Effects of biochar amendment on geotechnical properties of landfill cover soil. Waste Manage Res 33(6):524–532
Romero E, Gens A, Lloret A (1999) Water permeability, water retention and microstructure of unsaturated compacted Boom clay. Eng Geol 54(1–2):117–127
Su CC, Ma JF, Chen YP (2019) Biochar can improve the soil quality of new creation farmland on the Loess Plateau. Environ Sci Pollut R 26:2662–2670
Suliman W, Harsh JB, Abu-Lail NI, Fortuna AM, Dallmeyer I, Garcia-Pérez M (2017) The role of biochar porosity and surface functionality in augmenting hydrologic properties of a sandy soil. Sci Total Environ 574:139–147

Sun F, Lu S (2014) Biochars improve aggregate stability, water retention, and pore-space properties of clayey soil. J Plant Nutr Soil Sc 177(1):26–33

Tan X, Liu Y, Zeng G, Wang X, Hu X, Gu Y, Yang Z (2015) Application of biochar for the removal of pollutants from aqueous solutions. Chemosphere 125:70–85

Tan Z, Yuan S, Hong M, Zhang L, Huang Q (2020) Mechanism of negative surface charge formation on biochar and its effect on the fixation of soil Cd. J Hazard Mater 384:121370

Tomczyk A, Sokołowska Z, Boguta P (2020) Biochar physicochemical properties: pyrolysis temperature and feedstock kind effects. Rev Environ Sci Biotechnol 19:191–215

Turunen M, Hyväluoma J, Heikkinen J, Keskinen R, Kaseva J, Hannula M, Rasa K (2020) Quantifying the pore structure of different biochars and their impacts on the water retention properties of Sphagnum moss growing media. Biosyst Eng 191:96–106

Uzoma KC, Inoue M, Andry H, Zahoor A, Nishihara E (2011) Influence of biochar application on sandy soil hydraulic properties and nutrient retention. J Food Agric Environ 1137–1143

Vander Spoel D, Van Maaren PJ, Larsson P, Timneanu N (2006) Thermodynamics of hydrogen bonding in hydrophilic and hydrophobic media. J Phys Chem B 110:4393–4398

Vijayaraghavan K (2021) The importance of mineral ingredients in biochar production, properties and applications. Crit Rev Env Sci Tec 51(2):113–139

Wang H, Garg A, Huang S, Mei G (2020) Mechanism of compacted biochar-amended expansive clay subjected to drying–wetting cycles: Simultaneous investigation of hydraulic and mechanical properties. Acta Geophys 68:737–749

Wang J, Wang S (2019) Preparation, modification and environmental application of biochar: A review. J Clean Prod 227:1002–1022

Washburn RM (1921) What is a Fair Standard for Ice Cream? J Dairy Sci 4(3):231–239

Williams JH, Jones RA, Haley B, Kwok G, Hargreaves J, Farbes J, Torn MS (2021) Carbon-neutral pathways for the United States. AGU ADV 2(1):e2020AV000284

Wong JTF, Chow KL, Chen XW, Ng CWW, Wong MH (2022) Effects of biochar on soil water retention curves of compacted clay during wetting and drying. Biochar 4(1):1–14

Wong JTF, Chen Z, Chen X, Ng CWW, Wong MH (2017) Soil-water retention behavior of compacted biochar-amended clay: a novel landfill final cover material. J Soil Sediment 17:590–598

Wong JTF, Chen Z, Wong AYY, Ng CWW, Wong MH (2018) Effects of biochar on hydraulic conductivity of compacted kaolin clay. Environ Pollut 234:468–472

Xiao T, Li P, Pan ZH, Hou YF, Wang JD (2022) Relationship between water retention capacity and pore-size distribution of compacted loess. J Soil Sediment 1–15

Xu P, Qian H, Chen J, Wang L, Abliz X, He X, Ma G, Liu Y (2023a) New insights into microstructure evolution mechanism of compacted loess and its engineering implications. Bull Eng Geol Environ 82(1):36

Xu P, Qian H, Li S, Li W, Chen J, Liu Y (2023b) Geochemical evidence of fluoride behavior in loess and its influence on seepage characteristics: An experimental study. Sci Total Environ 882:163564

Xu X, Zhao Y, Sima J, Zhao L, Mašek O, Cao X (2017) Indispensable role of biochar-inherent mineral constituents in its environmental applications: A review. Bioresource Technol 241:887–899

Yang F, Zhao L, Gao B, Xu X, Cao X (2016) The interfacial behavior between biochar and soil minerals and its effect on biochar stability. Environ Sci Technol 50(5):2264–2271

Yi S, Chang NY, Imhoff PT (2020) Predicting water retention of biochar-amended soil from independent measurements of biochar and soil properties. Adv Water Resour 142:103638

Yuan JH, Xu RK, Zhang H (2011) The forms of alkalis in the biochar produced from crop residues at different temperatures. Bioresource Technol 102(3):3488–3497

Zapata CE, Houston WN, Houston SL, Walsh KD (2000) Soil-water characteristic curve variability. In: Shackelford, C.D., Houston, S.L., Chang, N.-Y. (Eds.), Advances in Unsaturated Geotechnics (GSP 99), Proceedings of the GeoDenver Conference, Denver, Colo., 5–8 August 2000. American Society of Civil Engineers, Reston, Va, pp. 84–124

Zhang YF, Wang JM, Feng Y (2021) The effects of biochar addition on soil physicochemical properties: A review. Catena 202:105284

Zhang YP, Gu K, Li JW, Tang CS, Shen ZT, Shi B (2020) Effect of biochar on desiccation cracking characteristics of clayey soils. Geoderma 364:114182

Zhao L, Cao X, Zheng W, Wang Q, Yang F (2015) Endogenous minerals have influences on surface electrochemistry and ion exchange properties of biochar. Chemosphere 136:133–139

Zong Y, Xiao Q, Lu S (2016) Acidity, water retention, and mechanical physical quality of a strongly acidic Ultisol amended with biochars derived from different feedstocks. J Soil Sediment 16:177–190